Atmospheric
Chemistry
and Physics

Highly oxygenated organic molecule (HOM) formation in the isoprene oxidation by NO₃ radical

Defeng Zhao[1,2,3,4], **Iida Pullinen**[2,a], **Hendrik Fuchs**[2], **Stephanie Schrade**[2], **Rongrong Wu**[2], **Ismail-Hakki Acir**[2,b],
Ralf Tillmann[2], **Franz Rohrer**[2], **Jürgen Wildt**[2], **Yindong Guo**[1], **Astrid Kiendler-Scharr**[2], **Andreas Wahner**[2],
Sungah Kang[2], **Luc Vereecken**[2], and **Thomas F. Mentel**[2]

[1]Department of Atmospheric and Oceanic Sciences & Institute of Atmospheric Sciences, Fudan University,
Shanghai, 200438, China
[2]Institute of Energy and Climate Research, IEK-8: Troposphere, Forschungszentrum Jülich, 52425 Jülich, Germany
[3]Big Data Institute for Carbon Emission and Environmental Pollution, Fudan University, Shanghai, 200438, China
[4]Institute of Eco-Chongming (IEC), 20 Cuiniao Rd., Chenjia Zhen, Chongming, Shanghai, 202162, China
[a]now at: Department of Applied Physics, University of Eastern Finland, Kuopio, 7021, Finland
[b]now at: Institute of Nutrition and Food Sciences, University of Bonn, 53115 Bonn, Germany

Correspondence: Thomas F. Mentel (t.mentel@fz-juelich.de) and Defeng Zhao (dfzhao@fudan.edu.cn)

Abstract. Highly oxygenated organic molecules (HOM) are found to play an important role in the formation and growth of secondary organic aerosol (SOA). SOA is an important type of aerosol with significant impact on air quality and climate. Compared with the oxidation of volatile organic compounds by ozone (O_3) and hydroxyl radical (OH), HOM formation in the oxidation by nitrate radical (NO_3), an important oxidant at nighttime and dawn, has received less attention. In this study, HOM formation in the reaction of isoprene with NO_3 was investigated in the SAPHIR chamber (Simulation of Atmospheric PHotochemistry In a large Reaction chamber). A large number of HOM, including monomers (C_5), dimers (C_{10}), and trimers (C_{15}), both closed-shell compounds and open-shell peroxy radicals (RO_2), were identified and were classified into various series according to their formula. Their formation pathways were proposed based on the peroxy radicals observed and known mechanisms in the literature, which were further constrained by the time profiles of HOM after sequential isoprene addition to differentiate first- and second-generation products. HOM monomers containing one to three N atoms (1–3N-monomers) were formed, starting with NO_3 addition to carbon double bond, forming peroxy radicals, followed by autoxidation. 1N-monomers were formed by both the direct reaction of NO_3 with isoprene and of NO_3 with first-generation products. 2N-monomers

(e.g., $C_5H_8N_2O_{n(n=7-13)}$, $C_5H_{10}N_2O_{n(n=8-14)}$) were likely the termination products of $C_5H_9N_2O_n\cdot$, which was formed by the addition of NO_3 to C5-hydroxynitrate ($C_5H_9NO_4$), a first-generation product containing one carbon double bond. 2N-monomers, which were second-generation products, dominated in monomers and accounted for $\sim 34\%$ of all HOM, indicating the important role of second-generation oxidation in HOM formation in the isoprene $+ NO_3$ reaction under our experimental conditions. H shift of alkoxy radicals to form peroxy radicals and subsequent autoxidation ("alkoxy–peroxy" pathway) was found to be an important pathway of HOM formation. HOM dimers were mostly formed by the accretion reaction of various HOM monomer RO_2 and via the termination reactions of dimer RO_2 formed by further reaction of closed-shell dimers with NO_3 and possibly by the reaction of $C5–RO_2$ with isoprene. HOM trimers were likely formed by the accretion reaction of dimer RO_2 with monomer RO_2. The concentrations of different HOM showed distinct time profiles during the reaction, which was linked to their formation pathway. HOM concentrations either showed a typical time profile of first-generation products, second-generation products, or a combination of both, indicating multiple formation pathways and/or multiple isomers. Total HOM molar yield was estimated to be $1.2\%^{+1.3\%}_{-0.7\%}$, which corresponded to a SOA yield of $\sim 3.6\%$

assuming the molecular weight of $C_5H_9NO_6$ as the lower limit. This yield suggests that HOM may contribute a significant fraction to SOA yield in the reaction of isoprene with NO_3.

1 Introduction

Highly oxygenated organic molecules (HOM) are an important class of compound formed in the oxidation of volatile organic compounds (VOC), including biogenic VOC (BVOC) and anthropogenic VOC (Crounse et al., 2013; Ehn et al., 2014; Jokinen et al., 2014; Rissanen et al., 2014; Jokinen et al., 2015; Krechmer et al., 2015; Mentel et al., 2015; Rissanen et al., 2015; Kenseth et al., 2018; Molteni et al., 2018; Garmash et al., 2020; McFiggans et al., 2019; Molteni et al., 2019; Quéléver et al., 2019). A number of recent studies have demonstrated that HOM play a pivotal role in both nucleation and also particle growth of pre-existing particles, thus contributing to secondary organic aerosol (SOA) (Ehn et al., 2014; Kirkby et al., 2016; Tröstl et al., 2016). Particularly, in the early stage of aerosol growth, HOM may contribute a significant fraction of SOA mass (Tröstl et al., 2016).

HOM are formed by the autoxidation of peroxy radicals (RO_2), which means they undergo intramolecular H shift forming alkyl radicals, followed by O_2 addition leading to formation of new RO_2 as shown below (Vereecken et al., 2007; Crounse et al., 2013; Ehn et al., 2017; Bianchi et al., 2019; Møller et al., 2019; Nozière and Vereecken, 2019; Vereecken and Nozière, 2020).

Besides autoxidation, the RO_2 can also react with HO_2, RO_2, and NO_3, either forming a series of termination products (Reactions R1–3), including organic hydroxyperoxide, alcohol, and carbonyl, or forming alkoxy radicals (RO, Reactions R4–5) via the following reactions.

$$RO_2 + R'O_2 \rightarrow ROH + R = O \qquad (R1)$$
$$RO_2 + R'O_2 \rightarrow R = O + R'OH \qquad (R2)$$
$$RO_2 + HO_2 \rightarrow ROOH \qquad (R3)$$
$$RO_2 + R'O_2 \rightarrow RO + R'O + O_2 \qquad (R4)$$
$$RO_2 + NO_3 \rightarrow RO + NO_2 + O_2 \qquad (R5)$$
$$RO_2 + R'O_2 \rightarrow ROOR' + O_2 \qquad (R6)$$
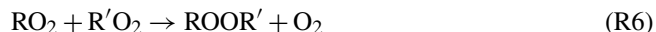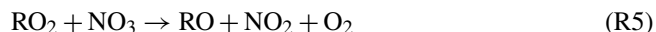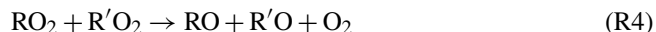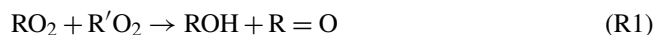
The termination products are detected in the mass spectra at masses $M + 1$, $M - 15$, and $M - 17$, respectively, with M being the molecular mass of the parent RO_2 (Ehn et al., 2014; Mentel et al., 2015). In case RO_2 is an acyl peroxy radical, percarboxylic acids and carboxylic acids are formed instead of hydroperoxides and alcohols in Reactions (R3) and (R1), respectively (Atkinson et al., 2006; Mentel et al., 2015). RO_2 can also form HOM dimers by the accretion reaction of two RO_2: Reaction (R6) (Berndt et al., 2018a, b; Valiev et al., 2019). Additionally, HOM can be formed via H shift in RO followed by O_2 addition (referred to as the "alkoxy-

proxy" pathway) (Finlayson-Pitts and Pitts, 2000; Vereecken and Peeters, 2010; Vereecken and Francisco, 2012; Mentel et al., 2015). These pathways are summarized in a recent comprehensive review (Bianchi et al., 2019), which also further clarifies HOM definition.

Currently, most laboratory studies of HOM formation focus on the VOC oxidation by OH and O_3 (Crounse et al., 2013; Ehn et al., 2014; Jokinen et al., 2014; Rissanen et al., 2014; Jokinen et al., 2015; Krechmer et al., 2015; Mentel et al., 2015; Rissanen et al., 2015; Kirkby et al., 2016; Tröstl et al., 2016; Kenseth et al., 2018; Molteni et al., 2018; Garmash et al., 2020; McFiggans et al., 2019; Molteni et al., 2019; Quéléver et al., 2019; Wang et al., 2020; Yan et al., 2020). HOM formation in the oxidation of VOC with NO_3 has received much less attention. NO_3 is another important oxidant of VOC mainly operating during nighttime. Particularly, NO_3 has high reactivity with unsaturated BVOC such as monoterpene and isoprene. It is often the dominant oxidant of these compounds at night, especially in regions where biogenic and anthropogenic emissions mix (Geyer et al., 2001; Brown et al., 2009, 2011). The reaction products contribute to SOA formation (Xu et al., 2015; Lee et al., 2016). Also, the organic nitrates produced in these reactions play an important role in nitrogen chemistry by altering NO_x concentration, which further influences photochemical recycling and ozone formation on the next day. Among these reaction products, HOM can also be formed (Xu et al., 2015; Lee et al., 2016; Yan et al., 2016). Despite the potential importance, studies of HOM formation in the oxidation of BVOC by NO_3 are still limited compared with the HOM formation via oxidation by O_3 and OH. Although a number of laboratory studies have investigated the reaction of NO_3 with BVOC (Ng et al., 2008; Fry et al., 2009; Rollins et al., 2009; Fry et al., 2011; Kwan et al., 2012; Fry et al., 2014; Boyd et al., 2015; Schwantes et al., 2015; Nah et al., 2016; Boyd et al., 2017; Claflin and Ziemann, 2018; Faxon et al., 2018; Draper et al., 2019; Takeuchi and Ng, 2019; Novelli et al., 2021; Vereecken et al., 2021), these studies mostly focus on either SOA yield and composition or on the gas-phase chemistry mechanism mainly for "traditional" oxidation products that stem from a few oxidation steps.

Importantly, HOM formation in the reaction of NO_3 with isoprene, the most abundant BVOC accounting for more than half of the global BVOC emissions, has not been explicitly addressed yet, to the best of our knowledge. Although isoprene from plants is mainly emitted under light conditions, i.e., in the daytime, isoprene can remain high after sunset in significant concentrations (Starn et al., 1998; Stroud et al., 2002; Brown et al., 2009) because of the reduced consumption by OH and is found to decay rapidly. A substantial fraction of isoprene can then be oxidized by NO_3 (Brown et al., 2009). Regarding the budget of NO_3, the reaction of isoprene with NO_3 can contribute a significant or even dominant fraction of NO_3 loss at night in regions where VOC is dominated by isoprene such as the northeastern US (Brown

et al., 2009). Under some circumstances, the reaction of isoprene with NO_3 can contribute a significant fraction during the afternoon and afterwards (Ayres et al., 2015; Hamilton et al., 2021). The reaction of isoprene with NO_3 is the subject of a number of studies (Ng et al., 2008; Perring et al., 2009; Rollins et al., 2009; Kwan et al., 2012; Schwantes et al., 2015; Vereecken et al., 2021). These studies focus on the oxidation mechanism and "traditional" oxidation products, as well as SOA yields. The initial step is the NO_3 addition to one of the $C = C$ double bounds, preferentially to the carbon C1 (Schwantes et al., 2015), followed by O_2 addition forming a nitrooxyalkyl peroxy radical (RO_2). This RO_2 can undergo the reactions described above, forming a series of products such as C5-nitrooxyhydroperoxide, C5-nitrooxycarbonyl, and C5-hydroxynitrate (Ng et al., 2008; Kwan et al., 2012) as well as methyl vinyl ketone (MVK), potentially methacrolein (MACR), formaldehyde, OH radical, and NO_2 as minor products (Schwantes et al., 2015). A high nitrate yield (57 %–95 %) was found (Perring et al., 2009; Rollins et al., 2009; Kwan et al., 2012; Schwantes et al., 2015). Products in the particle phase such as C_{10} dimers were also detected (Ng et al., 2008; Kwan et al., 2012; Schwantes et al., 2015). The SOA yield varies from 2 % to 23.8 % depending on the organic aerosol concentration (Ng et al., 2008; Rollins et al., 2009). These studies have provided valuable insights into oxidation mechanism, particle yield, and composition. However, because HOM formation was not the focus of these studies, only a limited number of products, mainly moderately oxygenated ones (oxygen number ≤ 2 in addition to NO_3 functional groups), were detected in the gas phase. The detailed mechanism of HOM formation and their yields in the reaction of BVOC+NO_3 are still unclear.

In this study, we investigated the HOM formation in the oxidation of isoprene by NO_3. We report the identification of HOM, including HOM monomers, dimers, and trimers. According to the reaction products and the literature, we discuss the formation mechanism of these HOM. The formation mechanism of various HOM is further constrained with time series of HOM upon repeated isoprene additions. We also provide an estimate of HOM yield in the isoprene + NO_3 reaction and assess their roles in SOA formation.

2 Experimental

2.1 Chamber setup and experiments

Experiments investigating the reaction of isoprene with NO_3 were conducted in the SAPHIR chamber (Simulation of Atmospheric PHotochemistry In a large Reaction chamber) at the Forschungszentrum Jülich, Germany. The details of the chamber have been described before (Rohrer et al., 2005; Zhao et al., 2015a, b, 2018). Briefly, SAPHIR is a Teflon chamber with a volume of 270 m^3. It can utilize natural sunlight for illumination and is equipped with a louvre system to switch between light and dark conditions. In this study, the experiments were conducted in the dark with the louvres closed.

Temperature and relative humidity were continuously measured. Gas- and particle-phase species were characterized using a comprehensive set of instruments with the details described before (Zhao et al., 2015b). VOC were characterized using a Proton Transfer Reaction Time-of-Flight Mass Spectrometer (PTR-ToF-MS, Ionicon Analytik, Austria). NO_x and O_3 concentrations were measured using a chemiluminescence NO_x analyzer (ECO PHYSICS TR480) and a UV photometer O_3 analyzer (ANSYCO, model O341M), respectively. OH, HO_2, and RO_2 concentrations were measured using a laser-induced fluorescence system (LIF) (Fuchs et al., 2012). NO_3 and N_2O_5 were detected by a custom-built instrument based on cavity ring-down spectroscopy. The design of the instrument is similar to that described by Wagner et al. (2011). NO_3 was directly detected in one cavity by its absorption at 662 nm and the sum of NO_3 and N_2O_5 in a second, heated cavity, which had a heated inlet to thermally decompose N_2O_5 to NO_3. The sampling flow rate was 3 to 4 L/min. The detection by cavity ring-down spectroscopy was achieved by a diode laser that was periodically switched on and off with a repetition rate of 200 Hz. Ring-down events were observed by a digital oscilloscope PC card during the time when the laser was switched off and were averaged over 1 s. The zero-decay time that is needed to calculate the concentration of NO_3 was measured every 20 s by chemically removing NO_3 in the reaction with excess nitric oxide (NO) in the inlet system. The accuracy of measurements was limited by the uncertainty in the correction for inlet losses of NO_3 and N_2O_5. In the case of N_2O_5 a transmission of (85 ± 10) % was achieved and, in the case of NO_3, (50 ± 30) %.

Before an experiment, the chamber was flushed with high-purity synthetic air (purity >99.9999 % O_2 and N_2). Experiments were conducted under dry conditions (RH < 2 %), and temperature was at 302 ± 3 K. NO_2 and O_3 were added to the chamber first to form N_2O_5 and NO_3, reaching concentrations of ~ 60 ppb for NO_2 and ~ 100 ppb for O_3. After around half an hour, isoprene was sequentially added into the chamber for three times at intervals of ~ 1 h. Around 40 min after the third isoprene injection, NO_2 was added to compensate for the loss of NO_3 and N_2O_5. Afterwards, three isoprene additions were repeated in the same way as before. O_3 was added before the fifth and sixth isoprene additions to compensate for its loss by reaction. The schematic for the experimental procedure is shown in Fig. S1. Experiments were designed such that the chemical system was dominated by the reaction of isoprene with NO_3 and the reaction of isoprene with O_3 did not play a major role (<3 % of the isoprene consumption). Figure S2 shows the relative contributions of the reaction of O_3 and NO_3 with isoprene to the total chemical loss of isoprene using the NO_3 and O_3 con-

centrations measured. The reaction with NO_3 accounted for $>95\%$ of the isoprene consumption for the whole experiment periods. The contribution of the reaction of isoprene with a trace amount of OH, mainly produced in the reaction of isoprene $+ O_3$ via Criegee intermediates (Nguyen et al., 2016), is negligible as the OH yield is less than one (Malkin et al., 2010), and thus its contribution is less than that of isoprene $+ O_3$. This is consistent with the contribution determined using measured OH concentration, despite some uncertainty in measured OH concentration due to the interference from NO_3. In these experiments, RO_2 fate is estimated to be dominated by its reaction with NO_3 according to the measured NO_3, RO_2, and HO_2 concentrations and their rate constants for the reactions with RO_2 (MCM v3.2; Jenkin et al., 1997, 2003; Saunders et al., 2003; Jenkin et al., 2015, via the website: http://mcm.leeds.ac.uk/MCM, last access: 1 November 2020 TS1) despite uncertainties in the measured RO_2 and HO_2 concentration due to interference from NO_3. As a large portion of RO_2 is not measured by LIF (Vereecken et al., 2021) and thus RO_2 is underestimated, we expected the reaction of $RO_2 + RO_2$ to also be important. Overall, we estimate that the RO_2 fate is dominated by the reaction $RO_2 + NO_3$ with a significant contribution of $RO_2 + RO_2$.

2.2 Characterization of HOM

In this study we refer to a similar definition for HOM by Bianchi et al. (2019); i.e., HOM typically contain six or more oxygen atoms formed via autoxidation and related chemistry of peroxy radicals. HOM were detected using a Chemical Ionization time-of-flight Mass Spectrometer (Aerodyne Research Inc., USA) with nitrate as the reagent ion (CIMS) (Eisele and Tanner, 1993; Jokinen et al., 2012). ^{15}N nitric acid was used to produce $^{15}NO_3^-$ in order to distinguish the NO_3 group into target molecules formed in the reaction from the reagent ion. The details of the instrument are described in our previous publications (Ehn et al., 2014; Mentel et al., 2015; Pullinen et al., 2020). The CIMS has a mass resolution of ~ 4000 (m/dm). Examples of peak fitting are shown in Fig. S3. HOM concentrations were estimated using the calibration coefficient of H_2SO_4 as described by Pullinen et al. (2020) because the charge efficiency of HOM and H_2SO_4 can be assumed to be equal and close to the collision limit (Ehn et al., 2014; Pullinen et al., 2020). The details of the calibration with H_2SO_4 are provided in Supplement Sect. S1. Since HOM contain more than six oxygen atoms and their clusters with nitrate ions are quite stable (Ehn et al., 2014), the charge efficiency of HOM is thus assumed to be equal to that of H_2SO_4, which is close to the collision limit (Viggiano et al., 1997). If HOM do not charge with nitrate ions at their collision limit or the clusters formed break during the short residence time in the charger, its concentration would be underestimated as pointed out by Ehn et al. (2014). Thus, our assumption provides a lower limit of the HOM concentration. The HOM yield was derived using the concentration of the HOM produced, divided by the concentration of isoprene that was consumed by NO_3. The uncertainty of HOM yield was estimated to $-55\%/+103\%$. The loss of HOM to the chamber was corrected using a wall loss rate of $6 \times 10^{-4}\,s^{-1}$ as quantified previously (Zhao et al., 2018). HOM concentrations were also corrected for dilution due to the replenishment flow needed to maintain a constant overpressure of the chamber (loss rate $\sim 1 \times 10^{-6}\,s^{-1}$) (Zhao et al., 2015b). The influence of wall loss correction and dilution correction on HOM yield was $\sim 12\%$ and $<1\%$, respectively. Although the wall loss rate of vapors in this study might not be exactly the same as in our previous photooxidation experiments (Zhao et al., 2018), HOM yield is not sensitive to the vapor wall loss rate. An increase in wall loss rate by 100% or a decrease by 50% only changes the HOM yield by 11% and -6%, respectively.

3 Results and discussion

3.1 Overview of HOM

The mass spectra of HOM in the gas phase formed in the oxidation of isoprene by NO_3 are shown in Fig. 1. A large number of HOM were detected. Almost all peaks are assigned HOM containing nitrogen atoms, with possibly few exceptions such as $C_5H_{10}O_8$ and $C_5H_8O_{11}$ with very minor peaks ($\lesssim 1\%$ of the maximum peak). The reaction products can be roughly divided into three classes: monomers (C5, ~ 200–400 Th), dimers (C10, ~ 400–600 Th), and trimers (C15, $\gtrsim 600$ Th), according to their mass-to-charge ratio (m/z). The detailed peak assignment of monomers, dimers, and trimers is discussed in the following sections.

3.2 HOM monomers and their formation

3.2.1 Overview of HOM monomers

HOM monomers showed a roughly repeating pattern in the mass spectrum at every 16 Th (corresponding to the mass of oxygen) (Fig. 1a). Here a number of series of HOM monomers with continuously increasing oxygenation were found, such as $C_5H_9NO_n$, $C_5H_7NO_n$, $C_5H_8N_2O_n$, and $C_5H_{10}N_2O_n$ (Tables 1 and S1–2 and Fig. 2). These monomers included both stable closed-shell molecules and open-shell radicals, such as $C_5H_8NO_n\cdot$ and $C_5H_9N_2O_n\cdot$. The open-shell molecules were likely RO_2 radicals because of their much longer lifetime and hence higher concentrations compared with alkoxy radicals (RO) and alkyl radicals (R). Since the observed stable products were mostly termination products of RO_2 reactions, we describe the stable products in a RO_2-oriented approach. It is worth noting that some of the termination products may contain multiple isomers formed from different pathways.
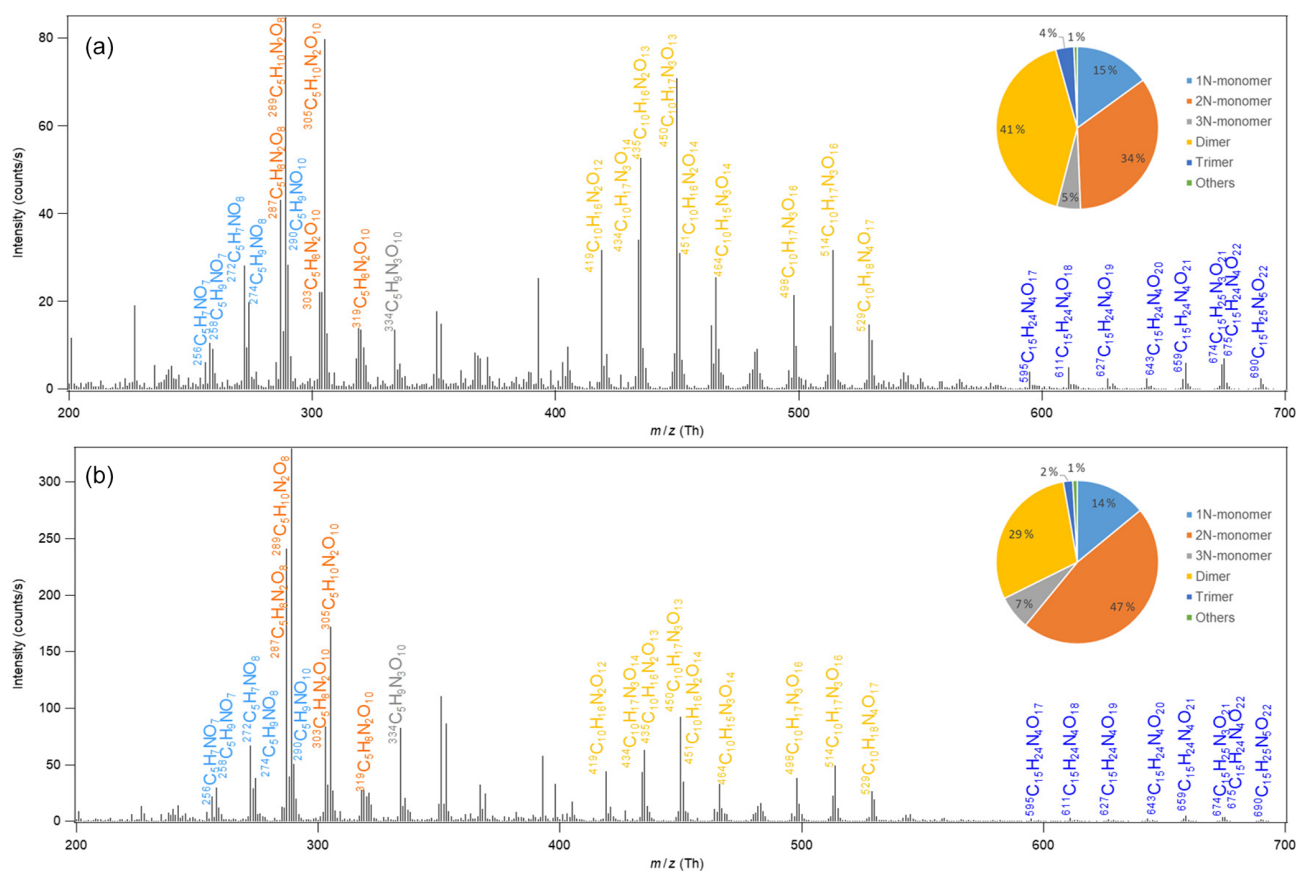
Figure 1. Mass spectrum of the HOM formed in the oxidation of isoprene by NO_3. HOM are detected as clusters with the reagent ion $^{15}NO_3^-$, which is not shown in the molecular formula in the figure for simplicity. Panels **(a)** and **(b)** show the average spectrum during the first isoprene addition period (P1) and for the whole period of six isoprene additions (P1–6), respectively. The insets show the contributions of different classes of HOM. 1–3N-monomer refers to the monomers containing one to three nitrogen atoms in the molecular formula.

Table 1. HOM monomers formed in the oxidation of isoprene by NO_3.

Series number	Product	Type[a]	Pathway of RO_2
M1a/b	$C_5H_8NO_{n(n=7–11)}$ $C_5H_9NO_{n(n=6–11)}$ $C_5H_7NO_{n(n=6–10)}$	RO_2 ROOH/ROH R=O	Isoprene+NO_3 Isoprene+NO_3+NO_3
M2a/b	$C_5H_9N_2O_{n(n=8–11,13,14)}$[b] $C_5H_{10}N_2O_{n(n=8–11,13,14)}$[b] $C_5H_8N_2O_{n(n=7–11)}$ $C_5H_9N_3O_{n(n=9–16)}$[b]	RO_2 ROOH/ROH R=O RO_2NO_2	Isoprene+NO_3+NO_3
M3	$C_5H_7N_2O_{n(n=9)}$ $C_5H_8N_2O_{n(n=8,9)}$ $C_5H_6N_2O_{n(n=8)}$	RO_2 ROOH/ROH R=O	Isoprene+NO_3+NO_3
M4	$C_5H_{10}NO_{n(n=8–9)}$ $C_5H_{11}NO_{n(n=7–9)}$ $C_5H_9NO_{n(n=7–8)}$	RO_2 ROOH/ROH R=O	Isoprene+NO_3+OH

[a] RO_2 denotes peroxy radical, and ROOH, ROH, R=O, and RO_2NO_2 denote the termination products containing hydroperoxy, hydroxyl, carbonyl group, and peroxynitrate, respectively.
[b] Peak assignment of compounds with $n = 13, 14$ may be subject to uncertainties.
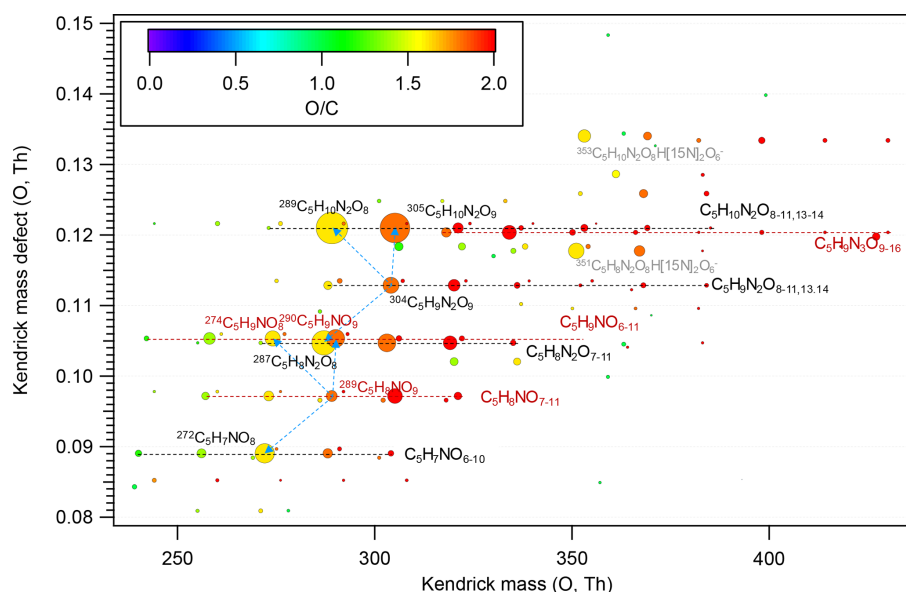
Figure 2. Kendrick mass defect plot for O of HOM monomers. The m/z in the molecular formula includes the reagent ion $^{15}NO_3^-$, which is not shown for simplicity. The size (area) of circles is set to be proportional to the average peak intensity of each molecular formula during the first isoprene addition period (P1). The species at m/z 351 and 353 (labeled in grey) are the adducts of $C_5H_8N_2O_8$ and $C_5H_{10}N_2O_8$ with $H[15N]_2O_6^-$, respectively. The blue dashed lines with arrows indicate the termination products hydroperoxide ($M+H$), alcohol ($M-O+H$), and ketone ($M-O-H$), with M the molecular formula of a HOM RO_2.

HOM monomers were classified into 1N-, 2N-, and 3N-monomers according to the number of nitrogen atoms that they contain. HOM without nitrogen atoms were barely observed except for very minor peaks ($\lesssim 1\%$ of the maximum peak) possibly assigned to $C_5H_{10}O_8$ and $C_5H_8O_{11}$. The contribution of 2N-monomers such as $C_5H_{10}N_2O_n$ and $C_5H_8N_2O_n$ was higher than that of the 1N-HOM monomers, and that of 3N-monomers was the lowest (Fig. 1, inset). The most abundant monomers were $C_5H_{10}N_2O_8$, $C_5H_{10}N_2O_9$, and $C_5H_8N_2O_8$. The termination products of $C_5H_9NO_8$, $C_5H_9NO_9$, and $C_5H_7NO_8$ also showed relatively high abundance. These limited numbers of compounds dominated the HOM monomers. Since 2N-monomers were second-generation products as discussed below, the higher-abundance 2N-monomers indicate that the second-generation HOM play an important role in the reaction of NO_3 with isoprene in the reaction conditions of our study, as also seen by Wu et al. (2020). This is more evident for the mass spectrum averaged over six isoprene addition periods (Fig. 1b), where the abundances of $C_5H_{10}N_2O_n$ and $C_5H_8N_2O_n$ were more dominant. This observation is in contrast with the finding for the reaction of O_3 with BVOC, which contains only one double bond such as α-pinene (Ehn et al., 2014), where HOM are mainly first-generation products formed via autoxidation. The higher abundance of HOM 2N-monomers than 1N-monomers is likely because HOM production rate via the autoxidation of 1N-monomer RO_2 following the reaction of isoprene with NO_3 may be slower than that of the reaction of 1N-monomers (including both HOM and non-HOM monomers) with NO_3. We would like to note that some less oxygenated 1N-monomers such as $C_5H_9NO_{4/5}$ and $C_5H_7NO_4$ may have high abundance but are not detected by NO_3^--CIMS and are not HOM and thus not included in HOM 1N-monomers.

3.2.2 1N-monomers

In our experiments we observed a $C_5H_8NO_n\bullet$ ($n = 7\text{--}12$) series (series M1) as well as its corresponding termination products $C_5H_7NO_{n-1}$, $C_5H_9NO_{n-1}$, and $C_5H_9NO_n$ via the reactions with RO_2 and HO_2, which contain carbonyl, hydroxyl, and hydroperoxy group, respectively. Overall, the peak intensities of $C_5H_9NO_n$ and $C_5H_7NO_n$ series first increased and then decreased as oxygen number increased (Fig. 2), with the peak intensity of $C_5H_9NO_8$ and $C_5H_7NO_8$ being the highest within their respective series when averaged over the whole experiment period.

$C_5H_8NO_n\bullet$ with odd numbers of oxygen atoms ($n = 7$, 9, 11, series M1a) were possibly formed by the attack of NO_3 to one double bond, preferentially to C1 according to previous studies (Skov et al., 1992; Berndt and Böge, 1997; Schwantes et al., 2015) and followed by autoxidation (Scheme 1a). We would like to note that NO_3^--CIMS only observed HOM with oxygen numbers ≥ 6 in this study due to its selectivity of detection. $C_5H_8NO_n\bullet$ with even numbers of oxygen atoms ($n = 8$, 10, series M1b in Table 1) were possibly formed after H shift of an alkoxy radical formed in Reactions (R4) or (R5) and subsequent O_2 addition ("alkoxy–peroxy" chan-

nel) (Scheme 1b), where the alkoxy radicals can be formed from both the $RO_2 + NO_3$ and $RO_2 + RO_2$ reactions. The hydroxy RO_2 formed can undergo further autoxidation, adding two oxygen atoms after each H shift. We would like to note that the scheme and other schemes in this study only show example isomers and pathways to form these molecules. It is likely that many of the reactions occurring are not the dominant channels as otherwise there would be much higher HOM yield as discussed below.

Some HOM monomers may contain multiple isomers and be formed via different pathways. For example, $C_5H_9NO_n$ can contain alcohols derived from RO_2 $C_5H_8NO_{n+1} \cdot$, hydroperoxides derived from RO_2 $C_5H_8NO_n \cdot$, or the ketones from $RO_2 C_5H_{10}NO_{n+1} \cdot$. Some RO_2 $C_5H_8NO_n \cdot$ may be formed via the reaction of first-generation products with NO_3 in addition to direct reaction of isoprene with NO_3. For example, $C_5H_8NO_7 \cdot$ can be formed by the reaction of NO_3 with $C_5H_8O_2$, which is a first-generation product observed previously in the reaction of isoprene with NO_3 or OH (Scheme S1b) (Kwan et al., 2012). Moreover, RO_2 $C_5H_8NO_n \cdot$ can be formed from C5-carbonylnitrate, a first-generation product, with OH (Scheme S1a). Trace amount of OH can be produced in the reaction of isoprene with NO_3 (Kwan et al., 2012; Wennberg et al., 2018). OH can also be formed via Criegee intermediates formed in the isoprene $+ O_3$ reaction (Nguyen et al., 2016), but this OH source was likely minor because the contribution of the isoprene $+ O_3$ reaction to total isoprene loss was negligible ($<5\%$, Fig. S2). In addition, $C_5H_8NO_8 \cdot$ may also be formed by the reaction of NO_3 with $C_5H_8O_3$, which is a first-generation product observed in the reaction of isoprene with OH (Kwan et al., 2012). The $C_5H_8NO_n \cdot$ formed via direct reaction of isoprene with NO_3 is a first-generation RO_2, while that formed via other indirect pathways is a second-generation RO_2. The time profiles of the isomers from these two pathways, however, are expected to be different, as will be discussed below.

Time series of HOM can shed light on their formation mechanisms. It is expected that first-generation products will increase quickly with isoprene addition and reach a maximum earlier in the presence of wall loss of organic vapor, while second-generation products will reach a maximum in the later stage or increase continuously if the production rate is higher than the loss rate. As a reference to analyze the time profiles of HOM, the time profiles of isoprene, NO_3, and N_2O_5 are also shown (Fig. S4). After isoprene was added in each period, NO_3 and N_2O_5 dropped dramatically and then gradually increased. We found that termination products within the same M1 series showed different time profiles. For example, in $C_5H_9NO_n$ series, $C_5H_9NO_8$ clearly increased instantaneously with isoprene addition and decreased quickly afterwards (Fig. 3a), indicating that it was a first-generation product, which was expected according to mechanism Scheme 1. $C_5H_9NO_6$ and $C_5H_9NO_{10}$ had a general increasing trend with time. While $C_5H_9NO_6$ increased

continuously with time, $C_5H_9NO_{10}$ reached maximum intensity in the late phase of each isoprene addition period and then decreased naturally or after isoprene addition. The faster loss of $C_5H_9NO_{10}$ than $C_5H_9NO_6$ may result from the faster wall loss due to its lower volatility. $C_5H_9NO_7$ and $C_5H_9NO_9$ showed a mixing time profile with features of the former two kinds of time profiles, increasing almost instantaneously with isoprene additions, especially in the first two periods, while increasing continuously or decreasing first with isoprene additions and then increasing later in each period. This kind of time series indicates that there were significant contributions from both first- and second-generation products.

The second-generation products may be different isomers formed in pathways other than shown in Scheme 1. Second-generation $C_5H_9NO_6$ can be formed via $C_5H_8NO_7 \cdot$, which can also be formed by the reaction of NO_3 and O_2 with $C_5H_8O_2$ as mentioned above (Scheme S2b) or by the reaction of OH with $C_5H_7NO_4$ (Scheme S2a). The time profiles of $C_5H_8NO_7 \cdot$ did show more contribution of second-generation processes because $C_5H_8NO_7 \cdot$ continuously increased with time in general. If the pathways via the reaction of NO_3 and O_2 with $C_5H_8O_2$ and the reaction of OH with $C_5H_7NO_4$ contribute most to $C_5H_9NO_6$, $C_5H_9NO_6$ would show mostly a time profile of second-generation products. Similarly, second-generation $C_5H_9NO_7$ can be formed via $C_5H_8NO_7 \cdot$ or $C_5H_8NO_8 \cdot$. The time series of $C_5H_8NO_8 \cdot$ did show the contribution of both the first- and second-generation processes, which generally increased with time while also responding to isoprene addition (Fig. S5). Similarly to $C_5H_9NO_6$, the second-generation pathways for $C_5H_9NO_7$, $C_5H_9NO_9$, and $C_5H_9NO_{10}$ are shown in Schemes S1, S3, and S4. For the RO_2 in $C_5H_8NO_n \cdot$ series other than $C_5H_8NO_{7/8} \cdot$, the peak of $C_5H_8NO_n \cdot$ overlaps with $C_5H_{10}N_2O_n$ in the mass spectra, which is a much larger peak and thus cannot be differentiated from $C_5H_{10}N_2O_n$. Therefore, it is not possible to obtain reliable separate time profiles in order to differentiate their major sources. It is worth noting that nitrate CIMS may not be able to detect all isomers of $C_5H_9NO_6$ due to the sensitivity limitation. Therefore, we cannot exclude the possibility that the absence of some first-generation isomers of $C_5H_9NO_6$ was due to the low sensitivity of these isomers.

Among the termination products of the 1N-monomer RO_2, carbonyl and hydroxyl/hydroperoxide species had comparable abundance in general (Table S1), suggesting that disproportionation reactions between RO_2 and RO_2 forming hydroxy and carbonyl species (R1–2) were likely an important RO_2 termination pathway. However, dependence of the exact ratio of carbonyl species to hydroxyl/hydroperoxide species on the number of oxygen atoms did not show a clear trend (Table S1), suggesting that the reactions of HOM RO_2 depended on their specific structure. There was no clear difference in the abundance between the termination products from $C_5H_8NO_n \cdot$ with odd and even numbers of oxygen atoms in general, although the most abundant termination prod-
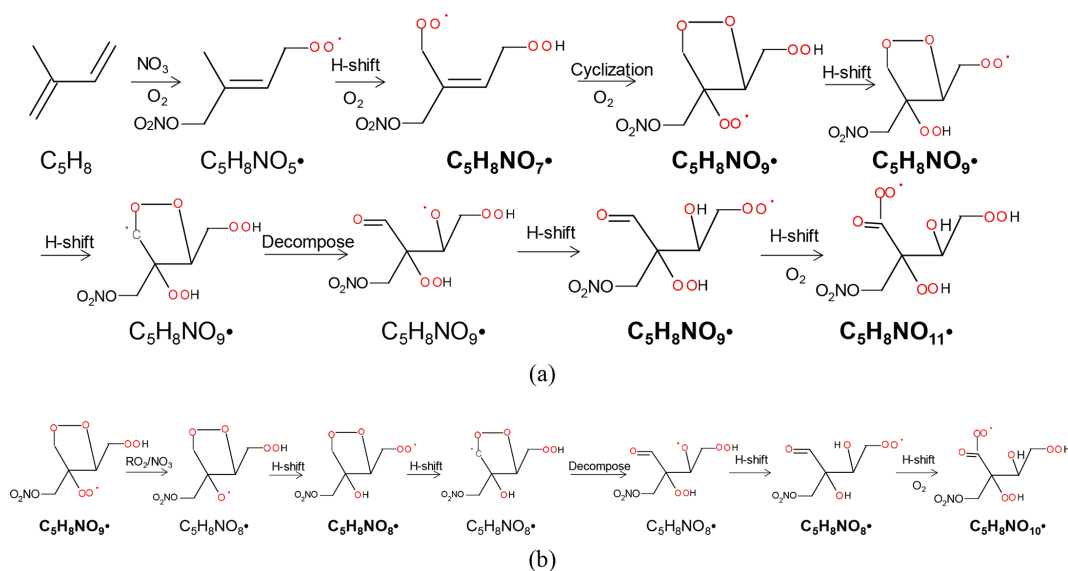
Scheme 1. The example pathways to form HOM RO_2 $C_5H_8NO_n\cdot$ ($n = 7, 9, 11$) series **(a)** and $C_5H_8NO_n\cdot$ ($n = 8, 10$) series **(b)** in the reaction of isoprene with NO_3. The detected products are in bold.

uct of $C_5H_8NO_n\cdot$, i.e., $C_5H_7NO_8$, was likely formed from $C_5H_8NO_9\cdot$ in series M1a. This fact indicates that both the peroxy pathway and alkoxy–peroxy pathway were important for the HOM formation in the isoprene + NO_3 reaction under our conditions, in agreement with the significant formation of alkoxy radicals from the reaction of RO_2 with NO_3 and RO_2.

In addition to the termination products of RO_2 M1, minor peaks of the RO_2 series $C_5H_{10}NO_n\cdot$ ($n = 8-9$) (M4, Table 1) and their corresponding termination products including hydroperoxide, alcohol, and carbonyl species were detected (Table S3). $C_5H_{10}NO_n$ were likely formed by sequential addition of NO_3 and OH to two double bonds of isoprene (Scheme S5). OH can react quickly with isoprene or with the first-generation products of the reaction of isoprene with NO_3, thus forming $C_5H_{10}NO_n\cdot$. In addition, a few very minor but noticeable peaks of $C_5H_9O_n\cdot$ and their corresponding termination products $C_5H_{10}O_n$ and $C_5H_8O_n$ were also observed. These HOM may be formed by the reactions of isoprene with trace amounts of OH and with O_3, although their contributions to reacted isoprene were negligible. These HOM were also observed in the reaction of isoprene with O_3 with and without OH scavengers (Jokinen et al., 2015).

Among 1N-monomer HOM, $C_5H_9NO_7$ has been observed in the particle phase using ESI-TOFMS by Ng et al. (2008), while others have not been observed in previous laboratory studies of the reaction of isoprene with NO_3, to our knowledge. A number of C_5 organic nitrates have been observed in field studies. For example, $C_5H_{7-11}NO_{6-8}$ and $C_5H_{7-11}NO_{4-9}$ have been observed in the gas phase (Massoli et al., 2018) and the particle phase (Lee et al., 2016; Chen et al., 2020), respectively, in a rural area of the southeastern US, where isoprene is abundant. Xu et al. (2021) observed a number of C_5 1N-HOM such as $C_5H_{7,9,11}NO_{6,7}$ in the polluted megacities of Nanjing and Shanghai of eastern China during summer. While many of these HOM have daytime sources and are attributed to photooxidation in the presence of NO_x, nighttime oxidation with NO_3 also contributed to their formation (Lee et al., 2016; Chen et al., 2020; Xu et al., 2021). $C_5H_{7-11}NO_{4-9}$ were also observed in chamber experiments of the reaction of isoprene with OH in the presence of NO_x (Lee et al., 2016). $C_5H_xNO_{4-9}$ and $C_5H_xNO_{4-10}$ have also been observed in the gas phase and particle phase, respectively, in a monoterpene-dominating rural area in southwestern Germany (Huang et al., 2019).

3.2.3   2N-mononmers

The 2N-monomer RO_2 series $C_5H_9N_2O_n\cdot$ ($n = 8-14$) were observed, as well as its likely termination products, $C_5H_8N_2O_n$ and $C_5H_{10}N_2O_n$, which contain a carbonyl and hydroxyl or hydroperoxide functional group, respectively. The RO_2 series $C_5H_9N_2O_n\cdot$ with an odd number of oxygen atoms ($n = 9, 11$) (M2a in Table 1) were likely formed from the first-generation product $C_5H_9NO_4$ (C5-hydroxynitrate) by adding NO_3 to the remaining double bond, forming $C_5H_9N_2O_9\cdot$, followed by autoxidation (Scheme 2a). This RO_2 series can also be formed by the addition of NO_3 to the double bond of first-generation products (e.g., $C_5H_9NO_5$, C5-nitrooxyhydroperoxide) and a subsequent alkoxy–peroxy step (Scheme 2b). $C_5H_9N_2O_n\cdot$ with an even number of oxygen atoms ($n = 8, 10, 12$) (M2b in Table 1) can be formed by the addition of NO_3 to the double bond of $C_5H_9NO_5$ followed by autoxidation (Scheme 3a) or of $C_5H_9NO_4$ followed by an alkoxy–peroxy step (Scheme 3b). The formation pathways of $C_5H_9N_2O_{13/14}\cdot$ and $C_5H_9N_2O_8\cdot$ cannot be
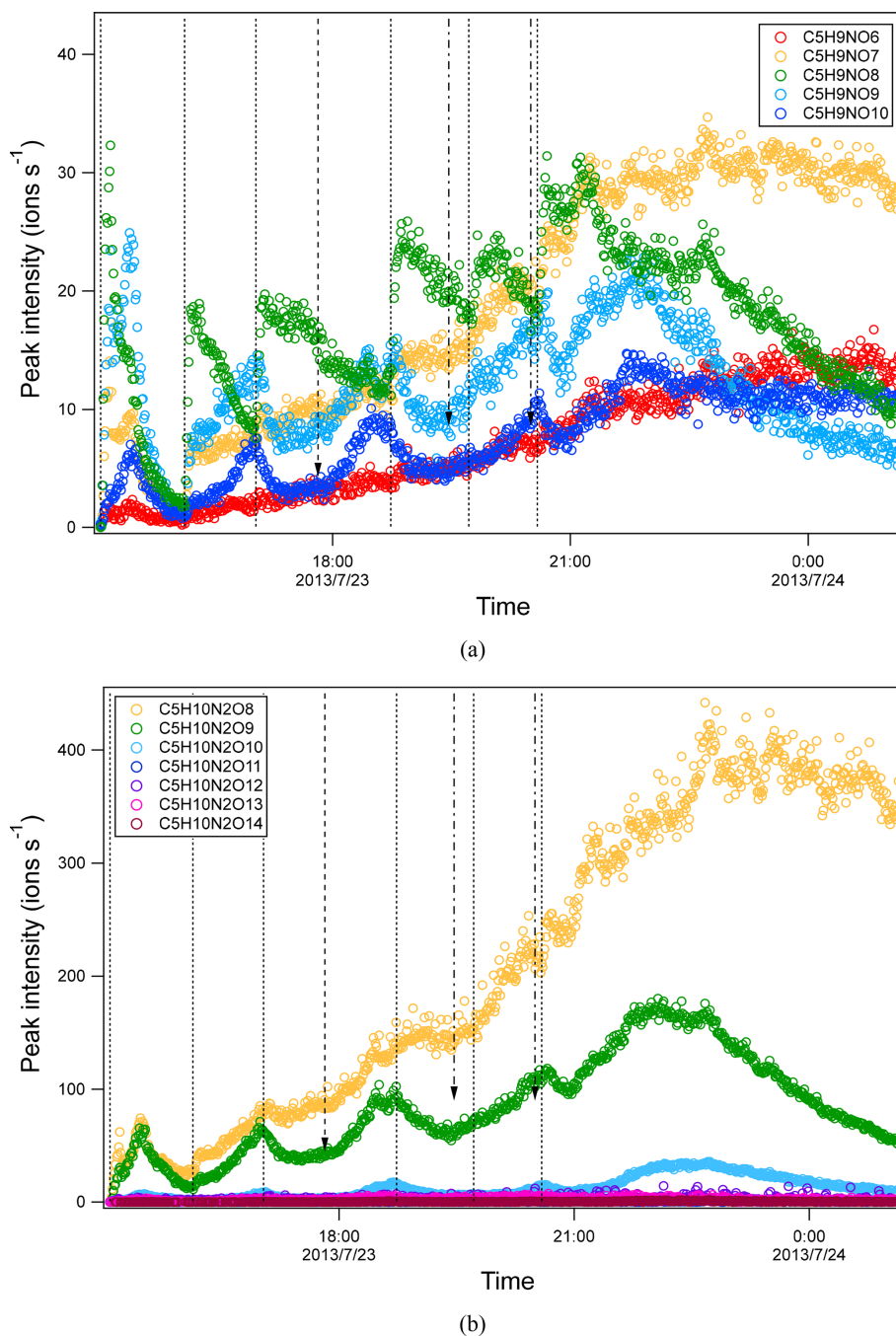
Figure 3. Time series of peak intensity of several HOM monomers of $C_5H_9NO_n$ series **(a)** and of $C_5H_{10}N_2O_n$ series **(b)**. They are likely the termination products of RO$_2$ $C_5H_8NO_n\cdot$ and $C_5H_9N_2O_n\cdot$, respectively. The dashed lines indicate the time of isoprene additions. The long-dashed arrow indicates the time of NO$_2$ addition. The dash-dotted arrows indicate the time of O$_3$ additions.

well explained, as they contain too many or too few oxygen atoms to be formed via the pathways in Scheme 2 or 3. In Schemes 2 and 3, we show the reactions starting from 1-NO$_3$-isoprene-4-OO as an example. In the Supplement, we have also shown the pathways starting from 1-NO$_3$-isoprene-2-OO peroxy radicals, which is indicated in a recent study by

Vereecken et al. (2021) to be the dominant RO$_2$ in the reaction of isoprene with NO$_3$.

Formation through either Scheme 2 or 3 means that $C_5H_8N_2O_n$ and $C_5H_{10}N_2O_n$ were second-generation products. The time series of $C_5H_{10}N_2O_n$ species clearly indicates that they were indeed second-generation products. $C_5H_{10}N_2O_n$ species generally did not increase immediately

(a)

(b)
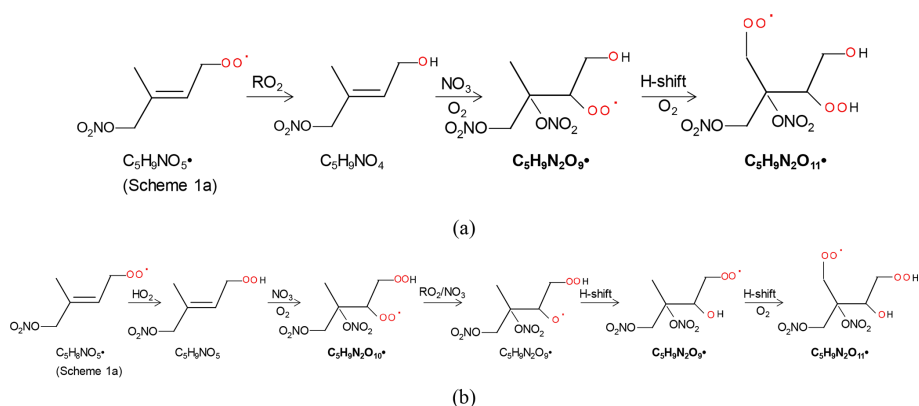
Scheme 2. The example pathways to form $C_5H_9N_2O_n$ ($n = 9, 11$) HOM RO_2 series by RO_2 channel **(a)** and alkoxy–peroxy channel. The detected products are in bold.

(a)

(b)
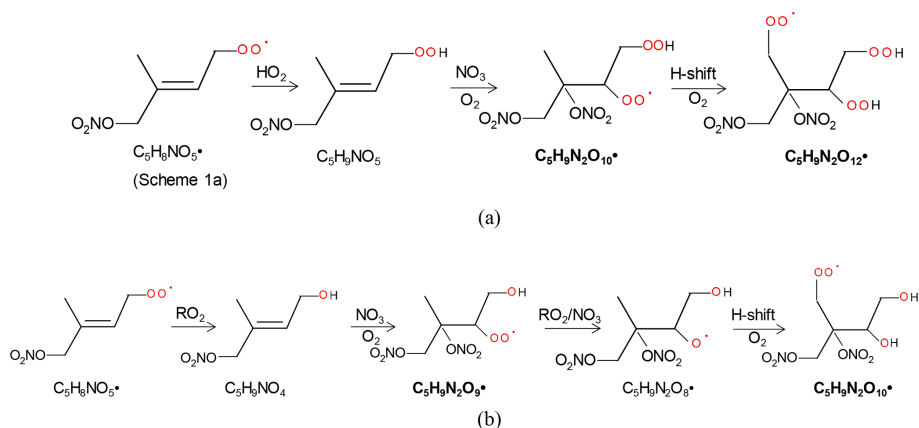
Scheme 3. The example pathways to form $C_5H_9N_2O_n$ ($n = 10, 12$) HOM RO_2 series by RO_2 channel **(a)** and alkoxy–peroxy channel **(b)**. The detected products are in bold.

with isoprene addition (Fig. 3b) but increased gradually with time and reached its maximum in the later stage of each period before decreasing with time (in periods 1 and 6) or decreasing after the next isoprene addition (periods 2–5). This time profile can be explained by the time series of the precursor of $C_5H_{10}N_2O_n$, $C_5H_9N_2O_n\cdot$ (RO_2) (Fig. S6). The changing rate (production rate minus destruction rate) of $C_5H_{10}N_2O_n$ concentration was dictated by the concentration of $C_5H_9N_2O_n\cdot$ and the wall loss rate. During periods 2 to 5, $C_5H_9N_2O_n\cdot$ gradually increased but decreased sharply after the isoprene additions, resulting from chemical reactions of $C_5H_9N_2O_n\cdot$ and additionally from wall loss. When the rate of change of the $C_5H_{10}N_2O_n$ concentration was positive, the concentration of $C_5H_{10}N_2O_n$ increased with time. After isoprene additions, the rate of change of the $C_5H_{10}N_2O_n$ concentration decreased dramatically to even negative, leading to decreasing concentrations. Similarly to $C_5H_{10}N_2O_n$, the $C_5H_8N_2O_n$ series did not respond immediately to isoprene additions (Fig. S7), which is expected for second-generation products according to the mechanism discussed

above (Schemes 2–3). Particularly, the continuing increase in $C_5H_8N_2O_n$ even after isoprene was completely depleted (at $\sim$ 21:40, Fig. S7) clearly indicates that these compounds were second-generation products, although in the end they decreased due to wall loss.

According to the finding by Ng et al. (2008), C5-hydroxynitrate decays much more quickly than C5-nitrooxyhydroperoxides. Additionally, C5-hydroxynitrate concentration is expected to be higher than that of nitrooxy-hydroperoxides because $RO_2 + RO_2$ forming alcohol is likely more important than $RO_2 + HO_2$ forming hydroperoxide in this study. Therefore, it is likely that $C_5H_9N_2O_n\cdot$ M2a series were mainly formed from $C_5H_9NO_4$ instead of $C_5H_9NO_5$, while $C_5H_9N_2O_n\cdot$ M2b were formed from $C_5H_9NO_4$ followed by an alkoxy–peroxy step. That is, Schemes 2a and 3b appear more likely.

Similarly to $C_5H_8NO_n\cdot$, the intensity of carbonyl species from $C_5H_9N_2O_n\cdot$ was also comparable with that of hydroxyl/hydroperoxide species, suggesting that $RO_2 + RO_2$ reaction forming ketone and alcohol was likely an impor-

tant pathway of HOM formation in the isoprene $+ NO_3$ reaction. In general, the intensities of the termination products from $C_5H_9N_2O_n\cdot$ with both even and odd oxygen numbers were comparable. This again suggests that both peroxy and alkoxy–peroxy pathways were important for HOM formation in the isoprene $+ NO_3$ reaction. The intensity of $C_5H_8N_2O_n$ first increased and then decreased with oxygen number, while $C_5H_{10}N_2O_n$ decreased with oxygen number, with $C_5H_{10}N_2O_8$ and $C_5H_8N_2O_8$ being the most abundant within their respective series.

Some 2N-monomers have been detected in previous studies of the reaction of isoprene with NO_3. $C_5H_{10}N_2O_8$ was detected in the particle phase by Ng et al. (2008), and $C_5H_8N_2O_7$ was detected in the gas phase by Kwan et al. (2012). $C_5H_9N_2O_9\cdot$ has been proposed to be formed via the pathway as in Scheme 2a (Ng et al., 2008), and it was directly detected in our study. $C_5H_8N_2O_7$ species has been proposed as a dinitrooxy epoxide formed by the oxidation of nitrooxyhydroperoxide (Kwan et al., 2012) instead of being a dinitrooxy ketone proposed in our study, a termination product of $C_5H_9N_2O_8\cdot$. Admittedly, $C_5H_8N_2O_7$ may contain both isomers. In addition, Ng et al. (2008) detected $C_5H_8N_2O_6$ in the gas phase, which was not detected in this study, likely due to the selectivity of NO_3^--CIMS. 2N-monomers have also been observed in previous field studies. For example, Massoli et al. (2018) observed $C_5H_{10}N_2O_{8-10}$ in rural Alabama, US, during the SOAS campaign. Xu et al. (2021) observed $C_5H_{8,10}N_2O_8$ and $C_5H_{10}N_2O_8$ in the polluted megacities of Nanjing and Shanghai during summer.

One could suppose that $C_5H_7N_2O_n\cdot$ should also be formed since C5-nitrooxycarbonyl ($C_5H_7NO_4$) also contains one double bond that can be attacked by NO_3 in a second oxidation step. However, concentrations of $C_5H_7N_2O_n$ were too low to assign molecular formulas with confidence except for $C_5H_7N_2O_9\cdot$, clearly showing that $C_5H_7N_2O_n\cdot$ was not important. This fact is consistent with the finding by Ng et al. (2008) that C5-nitrooxycarbonyls react slowly with NO_3. Additionally, the peroxy radical formed in the reaction of C5-nitrooxycarbonyls with NO_3 likely leads to more fragmentation in H shift as found in the OH oxidation of methacrolein (Crounse et al., 2012), which may also contribute to the low abundance of $C_5H_7N_2O_n$. The presence of HOM containing two N atoms is in line with the finding by Faxon et al. (2018), who detected products containing two N atoms in the reaction of NO_3 with limonene, which also contain two carbon double bonds. It is anticipated that for VOC with more than one double bond, NO_3 can add to all the double bonds as for isoprene and limonene.

3.2.4 3N-monomers

HOM containing three nitrogen atoms, $C_5H_9N_3O_n$ ($n = 9$–16), were observed. These compounds were possibly peroxynitrates formed by the reaction of RO_2 ($C_5H_9N_2O_n\cdot$) with NO_2. The time series of $C_5H_9N_3O_n$ was examined to check whether they match such a mechanism. If $C_5H_9N_3O_n$ were formed by the reaction of $C_5H_9N_2O_{n-2}\cdot$ with NO_2, the concentration would be a function of the concentrations of $C_5H_9N_2O_{n-2}\cdot$ and NO_2 as follows:

$$\frac{d[C_5H_9N_3O_n]}{dt} = k[C_5H_9N_2O_{n-2}\cdot][NO_2]$$
$$- k_{wall}[C_5H_9N_3O_n],$$

where $[C_5H_9N_3O_n]$, $[C_5H_9N_2O_{n-2}\cdot]$, and $[NO_2]$ are the concentrations of these species, k is the rate constant, and k_{wall} is the wall loss rate. Because the products of $C_5H_9N_2O_{n-2}\cdot$ and NO_2 were at their maximum at the end of each period and decreased rapidly after isoprene addition (Fig. S8), the concentration should have its maximum increasing rate at the end of each isoprene addition period. However, we found that only $C_5H_9N_3O_{12,15,16}$ showed such a time profile (Fig. S9), while $C_5H_9N_3O_{9,10,11,13,14}$ generally increased with time, different from what one would expect based on the proposed pathway. Therefore, it is likely that $C_5H_9N_3O_{12,15,16}$ were mainly formed via the reaction of $C_5H_9N_2O_n\cdot$ with NO_2, whereas $C_5H_9N_3O_{9,10,11,13,14}$ were not. Moreover, $C_5H_9N_3O_9$ cannot be explained by the reaction $C_5H_9N_2O_n\cdot$ ($n \geq 9$) with NO_2 or NO_3, because these reactions would add at least one more oxygen atom. One possible pathway to form $C_5H_9N_3O_9$ was the direct addition of N_2O_5 to the carbon double bond of C5-hydroxynitrate, forming a nitronitrate. Such a mechanism was proposed previously in the heterogeneous reaction of N_2O_5 with 1-palmitoyl-2-oleoyl-sn-glycero-3-phosphocholine (POPC) because $-NO_2$ and $-NO_3$ groups were detected (Lai and Finlayson-Pitts, 1991). This pathway generally matched the time series of $C_5H_9N_3O_{9,10,11,13,14}$ typical of second-generation products since C5-hydroxynitrate was a first-generation product. It is possible that the main pathway of $C_5H_9N_3O_{9,10,11,13,14}$ was the reaction of $C_5H_9NO_{4,5,6}$ with N_2O_5, although the reaction of N_2O_5 with C=C double bonds in common alkenes and unsaturated alcohols is believed to be unimportant (Japar and Niki, 1975; Pfrang et al., 2006).

3N-monomer, $C_5H_9N_3O_{10}$, has been observed in the particles formed in the isoprene $+ NO_3$ reaction by Ng et al. (2008). Here a complete series of $C_5H_9N_3O_n$ was observed. $C_5H_9N_3O_{10}$ was previously proposed to be formed by another pathway, i.e., the reaction of RO_2 ($C_5H_9N_2O_9\cdot$) and NO_3 (Ng et al., 2008). We further examined the possibility of such a pathway in our study. Similarly to NO_2, if $C_5H_9N_3O_n$ were formed by the reaction of $C_5H_9N_2O_{n-2}\cdot$ with NO_3, the concentration would have its maximum increasing rate at the end of each isoprene addition period. Among $C_5H_9N_2O_n\cdot$, the precursors of $C_5H_9N_3O_n$, $C_5H_9N_2O_{9,10,13,14}\cdot$ showed a maximum increasing rate and a subsequent decrease after isoprene addition. The difference in oxygen number between $C_5H_9N_3O_{12,15,16}$, the termination products, and $C_5H_9N_2O_{9,10,13,14}\cdot$, the corresponding RO_2 with the consistent time profile, is mostly two. Since

the reaction of $C_5H_9N_2O_n$ with NO_2 and NO_3 results in increased oxygen numbers by two and by one, respectively, we infer that it is more likely that $C_5H_9N_3O_{12,15,16}$ were formed by the reaction of $C_5H_9N_2O_{10,13,14}\cdot$ with NO_2 rather than NO_3, and thus they were likely peroxynitrates rather than nitrates formed by the reaction of RO_2 with NO_3. Since alkyl peroxynitrates decompose rapidly (Finlayson-Pitts and Pitts, 2000; Ziemann and Atkinson, 2012), it is possible that these compounds contained peroxyacylnitrates.

Little attention has been paid to the $RO_2 + NO_2$ pathway in nighttime chemistry of isoprene in the literature (Wennberg et al., 2018), which is likely due to the instability of the products. According to this pathway, $C_5H_8N_2O_n$, which was proposed as a ketone formed via $C_5H_9N_2O_9\cdot$ in the M2 series (Table 1) as discussed above, can also comprise peroxynitrate formed by the reaction of $C_5H_8NO_n\cdot$ (M1a RO_2) with NO_2. 3N dimers such as $C_5H_9N_3O_{10}$ have been observed in a recent field study in polluted cities in eastern China (Xu et al., 2021).

3.3   HOM dimers and their formation

A number of HOM dimer series were observed, including $C_{10}H_{16}N_2O_n$ ($n = 10$–17), $C_{10}H_{17}N_3O_n$ ($n = 11$–19), and $C_{10}H_{18}N_4O_n$ ($n = 15$–18), $C_{10}H_{18}N_2O_n$ ($n = 10$–16), $C_{10}H_{15}N_3O_n$ ($n = 13$–17), and $C_{10}H_{19}N_3O_n$ ($n = 14$–15) series (Tables 2, S3). $C_{10}H_{16}N_2O_n$ series (dimer 1, Table 2) was likely formed by the accretion reaction of two monomer RO_2 of M1a/b (Reaction R7).

$$C_5H_8NO_{n1}\cdot + C_5H_8NO_{n2}\cdot \rightarrow C_{10}H_{16}N_2O_{n1+n2-2} + O_2 \quad \text{(R7)}$$
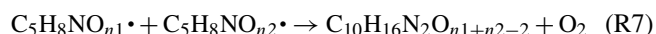
Similarly, $C_{10}H_{18}N_4O_n$ series (dimer 2, Table 2) were likely formed by the accretion reaction of two monomer RO_2 of M2 (Reaction R8). As $n1$ and $n2$ are ≥ 9, the number of oxygen in $C_{10}H_{18}N_4O_n$ is expected to be ≥ 16. This is consistent with our observation that only $C_{10}H_{18}N_4O_n$ with $n \geq 16$ had significant concentrations.

$$C_5H_9N_2O_{n1}\cdot + C_5H_9N_2O_{n2}\cdot \rightarrow C_{10}H_{18}N_4O_{n1+n2-2} + O_2 \quad \text{(R8)}$$
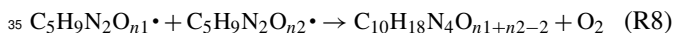
$C_{10}H_{17}N_3O_n$ series (dimer 3, Table 2) were likely formed by the cross-accretion reaction of one M1 RO_2 and one M2 RO_2 (Reaction R9). Since $n1$ is ≥ 5 and $n2$ is ≥ 9, the number of oxygen atoms in $C_{10}H_{17}N_3O_n$ is expected to be ≥ 12, which is also roughly consistent with our observation that only $C_{10}H_{17}N_3O_n$ with $n \geq 11$ were detected.

$$C_5H_8NO_{n1}\cdot + C_5H_9N_2O_{n2}\cdot \rightarrow C_{10}H_{17}N_3O_{n1+n2-2} + O_2 \quad \text{(R9)}$$
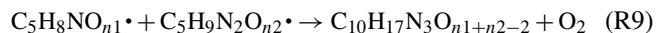
Similarly, $C_{10}H_{18}N_2O_{n(n=10-16)}$ and $C_{10}H_{15}N_3O_{n(n=13-17)}$ series (dimer 4, dimer 5, Table 2) were likely formed from the accretion reaction between one M1 RO_2 and one M4 RO_2 and between one M1 RO_2 and one M3 RO_2 ($C_5H_7N_2O_9\cdot$). Other dimer series than dimers 1–5 were also present. However, they had quite low intensity (Fig. 4), which was consistent with the low abundance of their parent monomer

RO_2. They can be formed from various accretion reactions of monomer RO_2. For example, $C_{10}H_{19}N_3O_n$ can be formed by the accretion reaction of $C_5H_9N_2O_n\cdot$ and $C_5H_{10}NO_n\cdot$ (Table 2).

Similarly to monomers, a few species dominated in the HOM dimer spectrum. The dominant dimer series were $C_{10}H_{17}N_3O_x$ and $C_{10}H_{16}N_2O_x$ series, with $C_{10}H_{17}N_3O_{12-14}$ and $C_{10}H_{16}N_2O_{12-14}$ showing the highest intensity among each series (Fig. 4). In addition, the O / C ratio or oxidation state of HOM dimers was generally lower than that of monomers (Figs. 2, 4), which resulted from the loss of two oxygen atoms in the accretion reaction of two monomer RO_2.

According to the mechanism above (Reactions R7–R9), we attempt to explain the relative intensities of the dimers using the signal intensities of monomer RO_2. Assuming that the rate constant for each of the HOM-RO_2 + HOM-RO_2 reactions forming dimers is the same considering that all HOM-RO_2 are highly oxygenated with a number of functional groups, it is expected that the dimer formed by the recombination between the most abundant RO_2 has the highest intensity. The most abundant monomers RO_2 were $C_5H_9N_2O_9\cdot$ and $C_5H_9N_2O_{10}\cdot$, and thus the most abundant dimers are expected to be $C_{10}H_{16}N_4O_{16}$, $C_{10}H_{16}N_4O_{17}$, and $C_{10}H_{16}N_4O_{18}$. This expected result is in contrast with our observation showing that the most abundant dimers were $C_{10}H_{17}N_3O_{12-14}$ and $C_{10}H_{16}N_2O_{12-14}$ (Fig. 4). The discrepancy is possibly attributed to the presence of less oxygenated RO_2 (with O ≤ 5) that have a low detection sensitivity in the NO_3-CIMS (Riva et al., 2019) due to their lower oxygenation compared with other HOM RO_2 shown above. These RO_2 may react with $C_5H_9N_2O_9\cdot$ and $C_5H_9N_2O_{10}\cdot$. For example, $C_5H_8NO_5\cdot$ (RO_2) is proposed as an important first-generation RO_2 in the oxidation of isoprene by NO_3 (Ng et al., 2008; Rollins et al., 2009; Kwan et al., 2012; Schwantes et al., 2015). Although $C_5H_8NO_5\cdot$ showed a very low signal in our mass spectra, it was likely to have high abundance since it was the first RO_2 formed in the reaction of isoprene with NO_3. Indeed, we found that the termination products of $C_5H_8NO_5\cdot$ such as $C_5H_9NO_5$, $C_5H_7NO_4$, and $C_5H_9NO_4$ had high abundance in another study, indicating the high abundance of $C_5H_8NO_5\cdot$. The accretion reaction of $C_5H_8NO_5\cdot$ with $C_5H_9N_2O_{9-10}\cdot$ and $C_5H_8NO_{9-10}\cdot$ can explain the high abundance of $C_{10}H_{17}N_3O_{12-14}$ and $C_{10}H_{16}N_2O_{12-14}$ among all dimers.

Provided that $C_5H_8NO_5\cdot$ is abundant, we still cannot explain the relative intensities of $C_{10}H_{17}N_3O_{12}$, $C_{10}H_{17}N_3O_{13}$, and $C_{10}H_{17}N_3O_{14}$ that were all formed by the accretion reaction with $C_5H_8NO_5\cdot$. $C_{10}H_{17}N_3O_{12}$ should have the highest intensity among $C_{10}H_{17}N_3O_{12-14}$ as its precursor RO_2, $C_5H_9N_2O_9\cdot$, is the most abundant. This suggests that accretion reactions other than those of $C_5H_8NO_5\cdot$ with $C_5H_9N_2O_{9-10}\cdot$ also contributed to $C_{10}H_{17}N_3O_{12-14}$. Admittedly, the assumption of different RO_2 having similar rate constants in accretion reactions may not be valid. For exam-

Table 2. HOM dimers and trimers formed in the oxidation of isoprene by NO_3.

Series number	Formula	Type	Pathway of RO_2
Dimer 1	$C_{10}H_{16}N_2O_{n(n=10-17)}$	ROOR[a]	M1[b] + M1
Dimer 2	$C_{10}H_{17}N_3O_{n(n=11-19)}$	ROOR	M1 + M2/M3 + M4
Dimer 3	$C_{10}H_{18}N_4O_{n(n=15-18)}$	ROOR	M2 + M2
Dimer 4	$C_{10}H_{18}N_2O_{n(n=10-16)}$	ROOR	M1 + M4
Dimer 5	$C_{10}H_{15}N_3O_{n(n=13-17)}$	ROOR	M1 + M3
Dimer 6	$C_{10}H_{19}N_3O_{n(n=14-15)}$	ROOR	M2 + M4
Dimer 7	$C_{10}H_{14}N_2O_{n(n=10-16)}$	ROOR	Unknown
Dimer 8	$C_{10}H_{15}NO_{n(n=9-12)}$	ROOR	$C_{10}H_{16}NO_n$
Dimer 9	$C_{10}H_{17}NO_{n(n=9-15)}$	ROOR	$C_{10}H_{16}NO_n$
Dimer R1	$C_{10}H_{16}N_3O_{n(n=12-15)}$	RO_2	Dimer 1 + NO_3
Dimer R2	$C_{10}H_{17}N_2O_{n(n=11-12)}$	RO_2	Dimer 1 + OH
Dimer R3	$C_{10}H_{17}N_4O_{n(n=16-18)}$	RO_2	Dimer 2 + NO_3
Dimer R4	$C_{10}H_{16}NO_{n(n=10-14)}$	RO_2	M1 + C_5H_8
Trimer 1	$C_{15}H_{24}N_4O_{n(n=17-22)}$	ROOR	Dimer R1 + M1
Trimer 2	$C_{15}H_{25}N_5O_{n(n=20-22)}$	ROOR	Dimer R3 + M1; dimer R1 + M2
Trimer 3	$C_{15}H_{25}N_3O_{n(n=13-20)}$	ROOR	Dimer R2 + M1; dimer R4 + M2
Trimer 4	$C_{15}H_{26}N_4O_{n(n=17-21)}$	ROOR	Dimer R2 + M2

[a] ROOR denotes organic peroxide. [b] The numbering refers to Table 1.
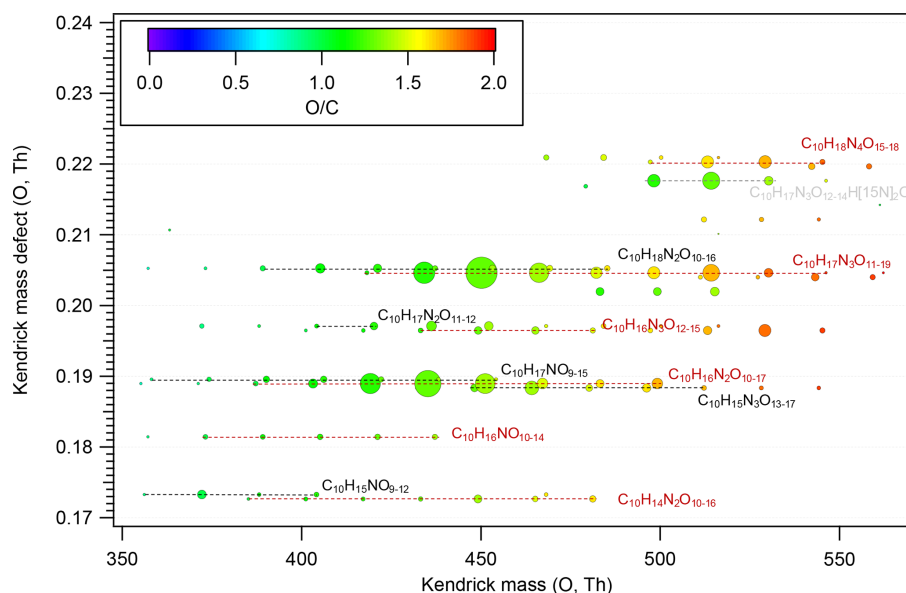
Figure 4. Kendrick mass defect plot for O of HOM dimers formed in the isoprene + NO_3 reaction. The size (area) of circles is set to be proportional to the average peak intensity of each molecular formula during the first isoprene addition period (P1). The molecular formula includes the reagent ion $^{15}NO_3^-$, which is not shown for simplicity. The species labeled in grey ($C_{10}H_{17}N_3O_{12-14}$ H$[15N]_2O_6^-$) are the adducts of $C_{10}H_{17}N_3O_{12-14}$ with H$[15N]_2O_6^-$.

ple, self-reaction of tertiary RO_2 is slower than secondary and primary RO_2 (Jenkin et al., 1998; Finlayson-Pitts and Pitts, 2000). Different rate constants may also lead to the observation that the most abundant dimers could not be explained by the most abundant RO_2.

The time profiles of $C_{10}H_{16}N_2O_n$ indicate contributions of both the first- and second-generation products. The dominance of the first- or second-generation products depended on the specific compounds. Most $C_{10}H_{16}N_2O_n$ compounds increased instantaneously after isoprene additions, indicating significant contributions of first-generation products. Since the formation of $C_{10}H_{16}N_2O_n$ likely involved $C_5H_8NO_5\cdot$ as discussed above, the instantaneous increase may result from the increase in $C_5H_8NO_5\cdot$ as well as other first-generation RO_2. After the initial increase, $C_{10}H_{16}N_2O_{10-12}$ then decayed with time (Fig. 5), while $C_{10}H_{16}N_2O_{13-15}$

increased again in the later phase of a period and when NO_2 and O_3 were added. The second increase indicated that $C_{10}H_{16}N_2O_{13-15}$ may contain more than one isomer, which had different production pathways. As discussed above, $C_5H_8NO_n\cdot$ can be either a first-generation RO_2 formed directly via the reaction of isoprene with NO_3 and autoxidation or a second-generation RO_2, e.g., formed via the reaction of $C_5H_8O_2$ with NO_3. Therefore, the second increase in $C_{10}H_{16}N_2O_{13-15}$ may result from the reaction of two first-generation RO_2 and of two second-generation RO_2 or between one first-generation and one second-generation RO_2. The increase in $C_{10}H_{16}N_2O_{14-15}$ after isoprene addition was not large, indicating the larger contributions from second-generation products compared with other $C_{10}H_{16}N_2O_n$. Overall, as the number of oxygen increased, the contribution of second-generation products to $C_{10}H_{16}N_2O_n$ increased.

In contrast to $C_{10}H_{16}N_2O_n$ series, $C_{10}H_{18}N_4O_n$ increased gradually after each isoprene addition and then decreased afterward (Fig. 6), either naturally or after isoprene additions, which is typical for second-generation products. Since $C_{10}H_{18}N_4O_n$ was likely formed by the accretion reaction of $C_5H_9N_2O_n\cdot$ (RO_2), the time profile of $C_{10}H_{18}N_4O_n$ was as expected since $C_5H_9N_2O_n\cdot$ was formed via the reaction of NO_3 with first-generation products $C_5H_9NO_n$. The $C_{10}H_{18}N_4O_n$ concentration depended on the product of the concentrations of two $C_5H_9N_2O_n\cdot$. Taking $C_{10}H_{18}N_4O_{16}$ as an example, its concentration can be expressed as follows:

$$\frac{d[C_{10}H_{18}N_4O_{16}]}{dt} = k[C_5H_9N_2O_9][C_5H_9N_2O_9] - k_{wl}[C_{10}H_{18}N_4O_{16}].$$

When the concentration of $C_5H_9N_2O_9\cdot$ increased, the changing rate of $C_{10}H_{18}N_4O_{16}$ was positive and increased, and thus the concentration of $C_{10}H_{18}N_4O_{16}$ increased. When the concentration $C_5H_9N_2O_9\cdot$ decreased sharply after isoprene additions, the changing rate of $C_{10}H_{18}N_4O_{16}$ decreased and even became negative values, and thus the concentration of $C_{10}H_{18}N_4O_{16}$ decreased after isoprene addition.

Similarly to the $C_{10}H_{16}N_2O_n$ series, while $C_{10}H_{17}N_3O_n$ first increased instantaneously with isoprene addition, it increased again during the later stage of each period (Fig. S10), showing a mixed behavior of the first-generation products and second-generation products. The time series of $C_{10}H_{17}N_3O_n$ was as expected in general because $C_{10}H_{17}N_3O_n$ was likely formed via the accretion reaction of $C_5H_8NO_n\cdot$ (M1 RO_2) and $C_5H_9N_2O_n\cdot$ (M2 RO_2), which were first- or second-generation, and second-generation RO_2, respectively.

Some dimers that cannot be explained by accretion reactions, such as $C_{10}H_{16}N_3O_{n(n=12-15)}\cdot$, $C_{10}H_{17}N_2O_{n(n=11-12)}\cdot$, $C_{10}H_{16}NO_{n(n=10-14)}\cdot$, $C_{10}H_{15}NO_{n(n=9-12)}$, and $C_{10}H_{17}NO_{n(n=9-15)}$, were also observed. These dimers had low abundance. We note that due to their low signals in the mass spectra, their assignment and thus range of n may be subject to uncertainties.

Since $C_{10}H_{16}NO_{n(n=10-16)}\cdot$, $C_{10}H_{16}N_3O_{n(n=12-15)}\cdot$, and $C_{10}H_{17}N_2O_n\cdot$ contain unpaired electrons, they cannot be formed via the direct accretion reaction of two RO_2. Instead, $C_{10}H_{16}N_3O_{n(n=12-15)}\cdot$ (dimer R1) and $C_{10}H_{17}N_2O_n\cdot$ (dimer R2) were likely RO_2 formed by the reaction of HOM dimers containing a double bond (dimer 1) with NO_3 and with OH, respectively, followed by the reaction with O_2.

$$C_{10}H_{16}N_2O_n + NO_3 + O_2 \rightarrow C_{10}H_{16}N_3O_n\cdot \qquad \text{(R10)}$$

$$C_{10}H_{16}N_2O_n + OH + O_2 \rightarrow C_{10}H_{17}N_2O_n\cdot \qquad \text{(R11)}$$
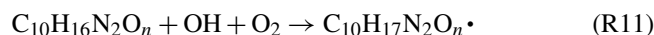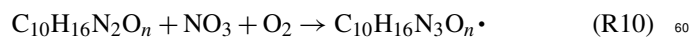
The corresponding termination products of $C_{10}H_{16}N_3O_n\cdot$ RO_2 series such as $C_{10}H_{15}N_3O_n$ (ketone) and $C_{10}H_{17}N_3O_n$ (hydroperoxide/alcohol) were also observed, although these compounds can also be formed via reactions between two RO_2 radicals (Reaction R9 and Table 1). Among the termination products, $C_{10}H_{15}N_3O_n$ had low intensity. Reaction (R13) and the termination reaction of $C_{10}H_{17}N_2O_n\cdot$ with HO_2 provided an additional pathway to $C_{10}H_{17}N_3O_n$ besides the Reaction (R9) pathway discussed above. Similarly, other dimers may also be formed by the termination reactions of dimer RO_2 with RO_2 or HO_2. For example, $C_{10}H_{18}N_4O_n$ can be formed via termination reaction of $C_{10}H_{17}N_4O_n\cdot$ with another RO_2 wherein $C_{10}H_{17}N_4O_n\cdot$ can be formed as follows.

$$C_{10}H_{17}N_3O_n + NO_3 + O_2 \rightarrow C_{10}H_{17}N_4O_n\cdot \qquad \text{(R12)}$$
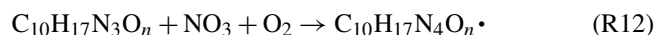
$C_{10}H_{16}NO_{n(n=10-14)}\cdot$ could be explained by the reaction of monomer RO_2 with isoprene.

$$C_5H_8NO_n\cdot + C_5H_8 + O_2 \rightarrow C_{10}H_{16}NO_n\cdot \qquad \text{(R13)}$$
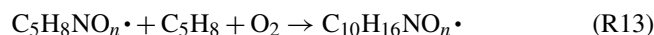
Only $C_{10}H_{16}NO_n\cdot$ with $n \geq 10$ were detected, while according to the mechanism of self-reaction between $C_5H_8NO_n\cdot$, the n range of $C_{10}H_{16}NO_n\cdot$ is expected to be 7–14. The absence of $C_{10}H_{16}NO_{n(n<10)}\cdot$ is likely attributed to their low abundance, which might result from low precursor concentrations, low reaction rates with isoprene, and/or faster reactive losses with other radicals. Such a reaction of RO_2 with isoprene has been proposed by Ng et al. (2008) and Kwan et al. (2012). The corresponding termination products of $C_{10}H_{16}NO_n\cdot$ are $C_{10}H_{15}NO_n$ (ketone) and $C_{10}H_{17}NO_n$ species (hydroperoxide/alcohol). $C_{10}H_{17}NO_n$ species showed a time profile of typical first-generation products (Fig. S11), i.e., increasing immediately with isoprene addition and then decaying with time. This behavior further supports the possibility of Reaction (R13). Yet the reaction rate of alkene with RO_2 is likely low due to the high activation energy (Stark, 1997, 2000). It is worth noting that to our knowledge no experimental kinetic data on the addition of RO_2 to alkenes in the gas phase in atmospheric relevant conditions are available, though fast, low-barrier ring closure reactions in unsaturated RO_2 radicals have been reported (Vereecken and Peeters, 2004, 2012; Kaminski et al., 2017; Richters et al., 2017; Chen et al., 2021). We would like
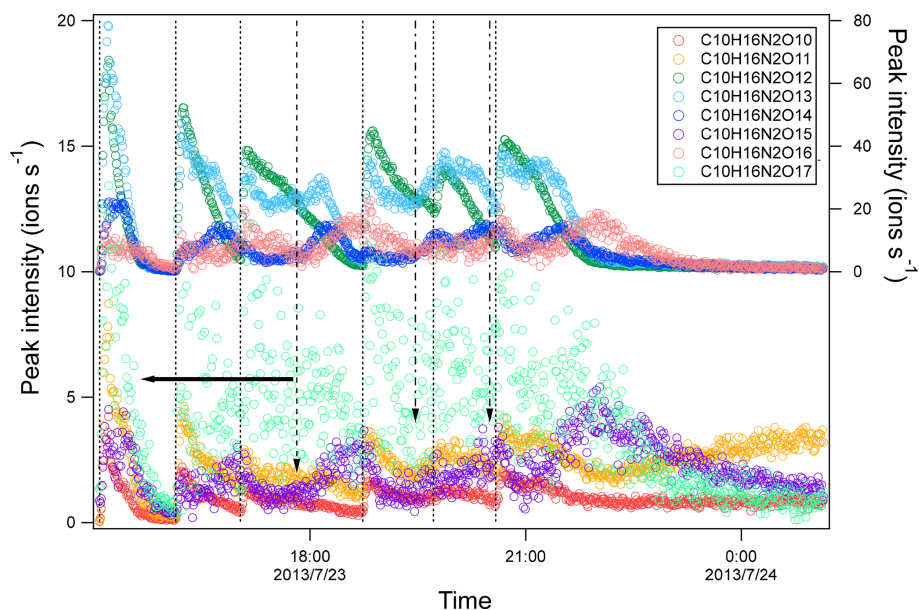
Figure 5. Time series of peak intensity of several HOM dimers of $C_{10}H_{16}N_2O_n$ series. The dashed lines indicate the time of isoprene additions. The long-dashed arrow indicates the time of NO_2 addition. The dash-dotted arrows indicate the time of O_3 additions. The horizontal arrows indicate y-axis scales for different markers.
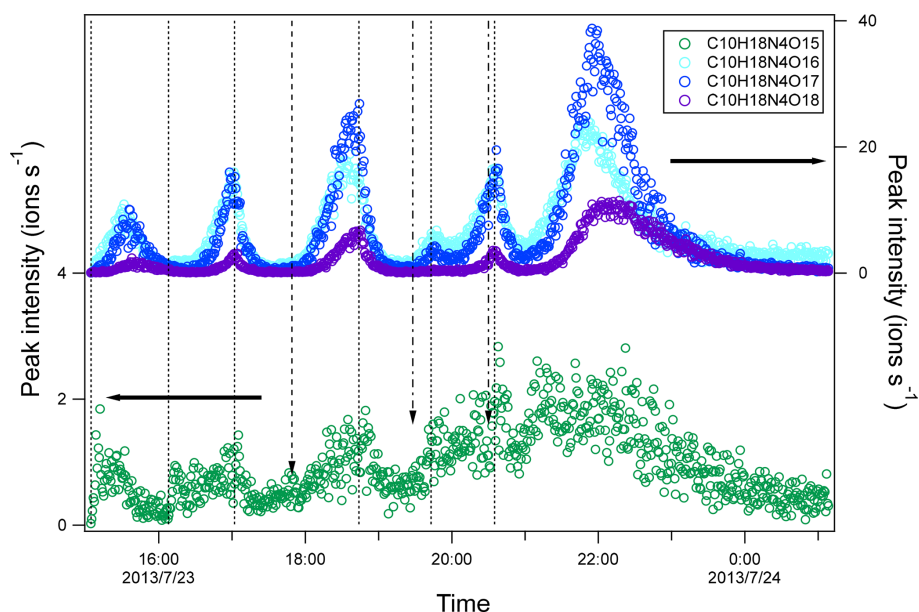
Figure 6. Time series of peak intensity of several HOM dimers of $C_{10}H_{18}N_4O_n$ series. The dashed lines indicate the time of isoprene additions. The long-dashed arrow indicates the time of NO_2 addition. The dash-dotted arrows indicate the time of O_3 additions. The horizontal arrows indicate y-axis scales for different markers.

to note that there is unlikely interference to C_{10}-HOM from monoterpenes, which has been reported previously (Bern-hammer et al., 2018), as the concentration of monoterpenes in the chamber during this study was below the limit of de-
5 tection, which was ~ 50 ppt (3σ).

Some of the dimers discussed above have been observed in previous laboratory studies. Ng et al. (2008)

found $C_{10}H_{16}N_2O_8$ and $C_{10}H_{16}N_2O_9$ in the gas phase and $C_{10}H_{17}N_3O_{12}$, $C_{10}H_{17}N_3O_{13}$, $C_{10}H_{18}N_4O_{16}$, and $C_{10}H_{17}N_5O_{18}$ in the particle phase. $C_{10}H_{16}N_2O_8$ and 10 $C_{10}H_{16}N_2O_9$ were also observed in our study, but their intensity in the MS was too low to assign molecular formulas with high confidence. The low intensity may be due to the low sensitivity of $C_{10}H_{16}N_2O_{8,9}$ in NO_3^--CIMS. Accord-

ing to modeling results of the products formed in cyclohexene ozonolysis by Hyttinen et al. (2015), at least two hydrogen bond donor functional groups are needed for a compound to be detected in a nitrate CIMS. As $C_{10}H_{16}N_2O_8$ and $C_{10}H_{16}N_2O_9$ have no and only one H-bond donor function groups, respectively, they are expected to have low sensitivity in NO_3^--CIMS. Moreover, the low intensity can be partly attributed to the much lower isoprene concentrations used in this study compared to previous studies, leading to the low concentration of $C_{10}H_{16}N_2O_8$ and $C_{10}H_{16}N_2O_9$ (Ng et al., 2008). $C_{10}H_{17}N_3O_{12}$, $C_{10}H_{17}N_3O_{13}$, $C_{10}H_{18}N_4O_{16}$, and $C_{10}H_{17}N_5O_{18}$ were all observed in the gas phase in this study, wherein the concentration of $C_{10}H_{17}N_5O_{18}$ was very low. The formation pathways of $C_{10}H_{17}N_3O_{12}$, $C_{10}H_{17}N_3O_{13}$, and $C_{10}H_{18}N_4O_{16}$ (Reaction R8) were generally similar to those proposed by Ng et al. (2008), except that the products from H shift of RO_2 were involved in the formation of $C_{10}H_{17}N_3O_{13}$. Among the two pathways of $C_{10}H_{18}N_4O_{16}$ formation (Reaction R8 and via Reaction R12), our results indicate that Reaction (R8) was the main pathway, based on the low concentrations of $C_{10}H_{17}N_4O_{16/17}$· and other termination products of them, $C_{10}H_{16}N_4O_{15/16}$. That the time profile of $C_{10}H_{18}N_4O_{16}$ was consistent with what is expected from Reaction (R8) as discussed above offers additional evidence for that conclusion.

Few field studies have reported HOM dimers formed via the reaction of NO_3 with isoprene. This might be because NO_3 + isoprene-HOM dimers can have the identical molecular formula to the HOM monomers from monoterpene oxidation. Possible contribution of dimer formation in the isoprene oxidation to C6–10 HOM in the particle phase observed at a rural site, Yorkville, US, is reported by Chen et al. (2020), although these HOM are thought to be more likely from monoterpene oxidation.

3.4 HOM trimers and their formation

A series of HOM trimers were observed, such as $C_{15}H_{24}N_4O_{n(n=17-22)}$, $C_{15}H_{25}N_5O_{n(n=20-22)}$, $C_{15}H_{25}N_3O_{n(n=13-20)}$, $C_{15}H_{26}N_4O_{n(n=17-21)}$, and $C_{15}H_{24}N_2O_{n(n=12-16)}$. Among the trimers, $C_{15}H_{24}N_4O_n$ was the most abundant series (Fig. S12). The $C_{15}H_{24}N_4O_n$ series can be explained by the accretion reaction of one monomer HOM RO_2 and one dimer HOM RO_2.

$$C_{10}H_{16}N_3O_{n1}\cdot + C_5H_8NO_{n2}\cdot$$
$$\rightarrow C_{15}H_{24}N_4O_{n1+n2-2} + O_2 \qquad (R14)$$
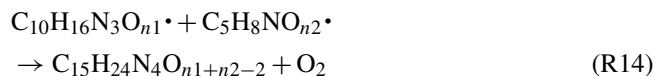
The formation pathways of dimer RO_2 $C_{10}H_{16}N_3O_n$ ($n = 12–15$) and $C_{10}H_{17}N_2O_n$ are shown above (Reactions R10 and R11).

The other trimers were likely formed via similar pathways (Table 2 and Supplement Sect. S2). Since NO_3^--CIMS cannot provide the structural information of these HOM trimers, we cannot elucidate the major pathways. However, in all these pathways, dimer-RO_2 is necessary to form a trimer, and most of the dimer-RO_2 formation pathways require at least one double bond in the dimer molecule except for the reaction of RO_2 with isoprene. Since one double bond has already reacted in the monomer-RO_2 formation, we anticipate that in the reaction with NO_3 it will be more favorable for precursors (VOC) containing more than one double bond to form trimer molecules than precursors containing only one double bond, as it is easier to generate new RO_2 radicals from these dimers by attack on the remaining double bond(s).

The time profile of $C_{15}H_{24}N_4O_n$ showed the mixed behavior of first- and second-generation products (Fig. S13), consistent with the mechanism discussed above since $C_5H_8NO_n$· and $C_{10}H_{16}N_3O_n$· were of first- or second-generation and second-generation, respectively. The contributions of the second-generation products became larger as the number of oxygen atoms increased. In contrast, $C_{15}H_{25}N_3O_n$ showed instantaneous increase with isoprene addition (Fig. S14), which was typical for time profiles of first-generation products. Both proposed formation pathways of $C_{15}H_{25}N_3O_n$ (Reactions RS6 and RS7) contained a second-generation RO_2, which was not in line with the time profile observed. The observation cannot be well explained unless we assume molecular adducts of a dimer with one monomer. It is also possible that some $C_{10}H_{17}N_2O_n$· were formed very, very quickly or that there were other formation pathways of $C_{15}H_{25}N_3O_n$ not accounted for here.

We are not aware of field studies reporting NO_3 + isoprene-HOM trimers, which is likely for the same reason for dimers discussed above. It is challenging to distinguish HOM trimers formed in the reaction NO_3 with isoprene from the dimers formed by cross-reaction of the RO_2 from monoterpene oxidation (C10-RO_2) with that from isoprene oxidation (C5-RO_2), as their molecular formulas can be identical.

3.5 Contributions of monomers, dimers, and trimers to HOM

The concentration (represented by peak intensity) of monomers was higher than that of dimers, but overall their concentrations remained on the same order of magnitude (Fig. 1a, inset). The concentration of trimers was much lower than that of monomers and dimers. The relative contributions of monomers, dimers, and trimers evolved in time due to the changing concentration of each HOM species. Comparing the contributions of various classes of HOM in period 1 with those in periods 1–6 reveals that the relative contribution of monomers increased with time, especially that of 2N-monomers, while the contribution of dimers decreased. This trend is attributed to the larger wall loss of dimers compared to monomers because of their lower volatility and also to the continuous formation of second-generation monomers, mostly 2N-monomers. Overall, the relative contribution of total HOM monomers decreased immediately after isoprene addition, while the contribution of HOM dimers increased

rapidly (Fig. S15), which was attributed to the faster increase in dimer intensity due to their rapid formation. Afterwards, the contribution of monomers to total HOM gradually increased and that of dimers decreased, which was partly due to the faster wall loss rate of dimers and to the continuous formation of second-generation monomers.

3.6 Yield of HOM

The HOM yield in the oxidation of isoprene by NO_3 was estimated using the sensitivity of H_2SO_4. It was derived for the first isoprene addition period to minimize the contribution of multi-generation products and to better compare with the data in the literature, thus denoted as primary HOM yield (Pullinen et al., 2020), and was estimated to be $1.2\%^{+1.3\%}_{-0.7\%}$. The uncertainty was estimated as shown in Supplement Sect. S1. Despite the uncertainty, the primary HOM yield here was much higher than the HOM yield from the ozonolysis and photooxidation of isoprene (Jokinen et al., 2015). The difference may be attributed to the more efficient oxygenation in the addition of NO_3 to carbon double bonds. Compared with the reaction with O_3 or OH, the initial peroxy radicals contain five oxygen atoms when isoprene reacts with NO_3, while the initial peroxy radicals contain only three oxygen atoms when reacting with OH, and the ozonide contains three oxygen atoms in the case of O_3.

4 Conclusion and implications

HOM formation in the reaction of isoprene with NO_3 was investigated in the SAPHIR chamber. A number of HOM monomers, dimers, and trimers containing one to five nitrogen atoms were detected, and their time-dependent concentration profiles were tracked throughout the experiment. Some formation mechanisms for various HOM were proposed according to the molecular formula identified and the available literature. HOM showed a variety of time profiles with multiple isoprene additions during the reaction. First-generation HOM increased instantaneously after isoprene addition and then decreased, while second-generation HOM increased gradually and then decreased with time, reaching a maximum concentration at the later stage of each period. The time profiles provide additional constraints on their formation mechanism besides the molecular formula, suggesting whether they were first-generation products or second-generation products or a combination of both. 1N-monomers (mostly C_5) were likely formed by NO_3 addition to a double bond of isoprene, forming monomer RO_2, followed by autoxidation and termination via the reaction with HO_2, RO_2, and NO_3. Time series suggest that some 1N-monomer could also be formed by the reaction of first-generation products with NO_3 and thus be of second generation. 2N-monomers were likely formed via the reaction of first-generation products such as C5-hydroxynitrate with

NO_3 and are thus second-generation products. 3N-monomers likely comprised peroxy/peroxyacyl nitrates formed by the reaction of 2N-monomer RO_2 with NO_2 and possibly nitronitrates formed via the direct addition of N_2O_5 to the first-generation products. HOM dimers were mostly formed by the accretion reactions between various HOM monomers RO_2, either first-generation or second-generation or with the contributions of both, and thus showed time profiles typical of either first-generation products, second-generation products, or a combination of both. Additionally, some dimer peroxy radicals (dimer RO_2) were formed by the reaction of NO_3 with dimers containing a C=C double bond. HOM trimers were proposed to be formed by accretion reactions between the monomer RO_2 and dimer RO_2.

Overall, both HOM monomers and dimers contribute significantly to total HOM, while trimers only contributed a minor fraction. Within both the monomer and dimer compounds, a limited set of compounds dominated the abundance, such as $C_5H_8N_2O_n$, $C_5H_{10}N_2O_n$, $C_{10}H_{17}N_3O_n$, and $C_{10}H_{16}N_2O_n$ series. 2N-monomers, which were second-generation products, dominated in monomers and accounted for $\sim 34\%$ of all HOM, indicating the important role of second-generation oxidation in HOM formation in the isoprene + NO_3 reaction. Both RO_2 autoxidation and "alkoxy–peroxy" pathways were found to be important for 1N- and 2N-HOM formation. In total, the yield of HOM monomers, dimers, and trimers accounted for $1.3\%^{+1.3\%}_{-0.7\%}$ of the isoprene reacted, which was much higher than the HOM yield in the oxidation of isoprene by OH and O_3 reported in the literature (Jokinen et al., 2015). This means that the reaction of isoprene with NO_3 is a competitive pathway of HOM formation from isoprene.

The HOM in the reaction of isoprene with NO_3 may account for a significant fraction of SOA. If all the HOM condense on particles, using the molecular weight of the HOM with the least molecular weight observed in this study ($C_5H_9NO_6$), the HOM yield corresponds to a SOA yield of 3.6%. Although SOA concentrations were not measured in this study, Ng et al. (2008) reported a SOA yield of the isoprene + NO_3 reaction of 4.3%–23.8%. Rollins et al. (2009) reported a SOA yield of 2% at low organic aerosol loading ($\sim 0.52\,\mu g\,m^{-3}$) and 14% if the further oxidation of the first-generation products is considered in the isoprene + NO_3 reaction. Comparing the potential SOA yield produced by HOM with SOA yields in the literature suggests that HOM may play an important role in the SOA formation in the isoprene + NO_3 reaction.

The RO_2 lifetime is approximately 20–50 s in our experiments, which is generally comparable to or shorter than the lifetime of RO_2 in the ambient atmosphere at night, varying from several tens to several hundreds of seconds (Fry et al., 2018), depending on the NO_3, HO_2, and RO_2 concentrations. Assuming a HO_2, RO_2, and NO_3 concentration of 5 ppt, 5 ppt (Tan et al., 2019), and 300 ppt (Brown and Stutz, 2012), respectively, the RO_2 lifetime in our study is

comparable to the nighttime RO_2 lifetime (50 s) found in urban locations and areas influenced by urban plume. In areas with longer RO_2 lifetime such as remote areas, the autoxidation is expected to be more important relative to bimolecular reactions. This may enhance HOM yield and thus enhance SOA yield. However, on the other hand, at lower RO_2 concentration and thus longer RO_2 lifetime, reduced rates of $RO_2 + RO_2$ reactions producing low-volatility dimers can reduce the SOA yield by reducing dimer yield (McFiggans et al., 2019; Pullinen et al., 2020). The RO_2 fate in our experiments is dominated the reaction $RO_2 + NO_3$ with significant contribution of $RO_2 + RO_2$, which can also represent the RO_2 fate in the urban areas and areas influenced by urban plume. Our experiment condition cannot represent the chemistry in HO_2-dominated regions such as clean forest environments (Schwantes et al., 2015).

We observed the second-generation products formed by the reaction of first-generation products. The lifetime of first-generation nitrates in the ambient atmosphere, according their rate constants with OH and NO_3 (Wennberg et al., 2018), are ~ 5 and ~ 1.3–4 h, respectively, with respect to the reaction with OH and NO_3 assuming a typical OH concentration of 2×10^6 molec. cm^{-3} (Lu et al., 2014; Tan et al., 2019) and a NO_3 concentration of 100–300 ppt in urban areas (Brown and Stutz, 2012). Therefore, they have the chance to react further with OH and NO_3 at dawn. In our experiments, the lifetimes of these first-generation nitrates with respect to OH and NO_3 are comparable to the aforementioned lifetime due to comparable OH and NO_3 concentrations with these ambient conditions. Therefore, our findings on the second-generation products are relevant to the ambient urban atmosphere and areas influenced by urban plumes. Some of these products such as $C_5H_{8,10}N_2O_8$ and multi-generation nitrooxyorganosulfates have been observed in recent field studies in polluted megacities in eastern China (Hamilton et al., 2021; Xu et al., 2021).

Data availability. All the data in the figures of this study are available upon request to the corresponding author (t.mentel@fz-juelich.de or dfzhao@fudan.edu.cn).

Supplement. The supplement related to this article is available online at: https://doi.org/10.5194/acp-21-1-2021-supplement.

Author contributions. TFM, HF, StS, DZ, IP, AW, and AKS designed the experiments. Instrument deployment and operation were carried out by IP, HF, StS, IHA, RT, FR, DZ, and RW. Data analysis was done by DZ, HF, StS, RW, IHA, RT, FR, YG, SK, DZ, TFM, RW, JW, and SK, and LV interpreted the compiled data set. DZ and TFM wrote the paper. All the co-authors discussed the results and commented on the paper.

Competing interests. The authors declare that they have no conflict of interest.

Special issue statement. This article is part of the special issue "Simulation chambers as tools in atmospheric research (AMT/ACP/GMD inter-journal SI)". It is not associated with a conference.

Acknowledgements. We thank the SAPHIR team for supporting our measurements and providing helpful data. Defeng Zhao and Yindong Guo would like to thank the National Natural Science Foundation of China (41875145). We would like to thank three anonymous reviewers and Kristian Møller for their helpful comments.

Financial support. This research has been supported by the National Natural Science Foundation of China (grant no. 41875145).

The article processing charges for this open-access publication were covered by the Forschungszentrum Jülich.

Review statement. This paper was edited by Nga Lee Ng and reviewed by three anonymous referees.

References

Atkinson, R., Baulch, D. L., Cox, R. A., Crowley, J. N., Hampson, R. F., Hynes, R. G., Jenkin, M. E., Rossi, M. J., Troe, J., and IUPAC Subcommittee: Evaluated kinetic and photochemical data for atmospheric chemistry: Volume II – gas phase reactions of organic species, Atmos. Chem. Phys., 6, 3625–4055, https://doi.org/10.5194/acp-6-3625-2006, 2006.

Ayres, B. R., Allen, H. M., Draper, D. C., Brown, S. S., Wild, R. J., Jimenez, J. L., Day, D. A., Campuzano-Jost, P., Hu, W., de Gouw, J., Koss, A., Cohen, R. C., Duffey, K. C., Romer, P., Baumann, K., Edgerton, E., Takahama, S., Thornton, J. A., Lee, B. H., Lopez-Hilfiker, F. D., Mohr, C., Wennberg, P. O., Nguyen, T. B., Teng, A., Goldstein, A. H., Olson, K., and Fry, J. L.: Organic nitrate aerosol formation via NO_3 + biogenic volatile organic compounds in the southeastern United States, Atmos. Chem. Phys., 15, 13377–13392, https://doi.org/10.5194/acp-15-13377-2015, 2015.

Berndt, T. and Böge, O.: Gas-phase reaction of NO_3 radicals with isoprene: a kinetic and mechanistic study, Int. J. Chem. Kinet., 29, 755–765, https://doi.org/10.1002/(sici)1097-4601(1997)29:10<755::Aid-kin4>3.0.Co;2-l, 1997.

Berndt, T., Mender, B., Scholz, W., Fischer, L., Herrmann, H., Kulmala, M., and Hansel, A.: Accretion Product Formation from Ozonolysis and OH Radical Reaction of alpha-Pinene: Mechanistic Insight and the Influence of Isoprene and Ethylene, Environ. Sci. Technol., 52, 11069–11077, https://doi.org/10.1021/acs.est.8b02210, 2018a.

Berndt, T., Scholz, W., Mentler, B., Fischer, L., Herrmann, H., Kulmala, M., and Hansel, A.: Accretion Product For-

mation from Self- and Cross-Reactions of RO$_2$ Radicals in the Atmosphere, Angew. Chem.-Int. Edit., 57, 3820–3824, https://doi.org/10.1002/anie.201710989, 2018b.

Bernhammer, A.-K., Fischer, L., Mentler, B., Heinritzi, M., Simon, M., and Hansel, A.: Production of highly oxygenated organic molecules (HOMs) from trace contaminants during isoprene oxidation, Atmos. Meas. Tech., 11, 4763–4773, https://doi.org/10.5194/amt-11-4763-2018, 2018.

Bianchi, F., Kurten, T., Riva, M., Mohr, C., Rissanen, M. P., Roldin, P., Berndt, T., Crounse, J. D., Wennberg, P. O., Mentel, T. F., Wildt, J., Junninen, H., Jokinen, T., Kulmala, M., Worsnop, D. R., Thornton, J. A., Donahue, N., Kjaergaard, H. G., and Ehn, M.: Highly Oxygenated Organic Molecules (HOM) from Gas-Phase Autoxidation Involving Peroxy Radicals: A Key Contributor to Atmospheric Aerosol, Chem. Rev., 119, 3472–3509, https://doi.org/10.1021/acs.chemrev.8b00395, 2019.

Boyd, C. M., Sanchez, J., Xu, L., Eugene, A. J., Nah, T., Tuet, W. Y., Guzman, M. I., and Ng, N. L.: Secondary organic aerosol formation from the β-pinene+NO$_3$ system: effect of humidity and peroxy radical fate, Atmos. Chem. Phys., 15, 7497–7522, https://doi.org/10.5194/acp-15-7497-2015, 2015.

Boyd, C. M., Nah, T., Xu, L., Berkemeier, T., and Ng, N. L.: Secondary Organic Aerosol (SOA) from Nitrate Radical Oxidation of Monoterpenes: Effects of Temperature, Dilution, and Humidity on Aerosol Formation, Mixing, and Evaporation, Environ. Sci. Technol., 51, 7831–7841, https://doi.org/10.1021/acs.est.7b01460, 2017.

Brown, S. S. and Stutz, J.: Nighttime radical observations and chemistry, Chem. Soc. Rev., 41, 6405–6447, https://doi.org/10.1039/c2cs35181a, 2012.

Brown, S. S., deGouw, J. A., Warneke, C., Ryerson, T. B., Dubé, W. P., Atlas, E., Weber, R. J., Peltier, R. E., Neuman, J. A., Roberts, J. M., Swanson, A., Flocke, F., McKeen, S. A., Brioude, J., Sommariva, R., Trainer, M., Fehsenfeld, F. C., and Ravishankara, A. R.: Nocturnal isoprene oxidation over the Northeast United States in summer and its impact on reactive nitrogen partitioning and secondary organic aerosol, Atmos. Chem. Phys., 9, 3027–3042, https://doi.org/10.5194/acp-9-3027-2009, 2009.

Brown, S. S., Dube, W. P., Peischl, J., Ryerson, T. B., Atlas, E., Warneke, C., de Gouw, J. A., Hekkert, S. t. L., Brock, C. A., Flocke, F., Trainer, M., Parrish, D. D., Feshenfeld, F. C., and Ravishankara, A. R.: Budgets for nocturnal VOC oxidation by nitrate radicals aloft during the 2006 Texas Air Quality Study, J. Geophys. Res.-Atmos., 116, D24305, https://doi.org/10.1029/2011jd016544, 2011.

Chen, J., Møller, K. H., Wennberg, P. O., and Kjaergaard, H. G.: Unimolecular Reactions Following Indoor and Outdoor Limonene Ozonolysis, J. Phys. Chem. A, 125, 669–680, 10.1021/acs.jpca.0c09882, 2021.

Chen, Y., Takeuchi, M., Nah, T., Xu, L., Canagaratna, M. R., Stark, H., Baumann, K., Canonaco, F., Prévôt, A. S. H., Huey, L. G., Weber, R. J., and Ng, N. L.: Chemical characterization of secondary organic aerosol at a rural site in the southeastern US: insights from simultaneous high-resolution time-of-flight aerosol mass spectrometer (HR-ToF-AMS) and FIGAERO chemical ionization mass spectrometer (CIMS) measurements, Atmos. Chem. Phys., 20, 8421–8440, https://doi.org/10.5194/acp-20-8421-2020, 2020.

Claflin, M. S. and Ziemann, P. J.: Identification and Quantitation of Aerosol Products of the Reaction of β-Pinene with NO$_3$ Radicals and Implications for Gas- and Particle-Phase Reaction Mechanisms, J. Phys. Chem. A, 122, 3640–3652, https://doi.org/10.1021/acs.jpca.8b00692, 2018.

Crounse, J. D., Knap, H. C., Ørnsø, K. B., Jørgensen, S., Paulot, F., Kjaergaard, H. G., and Wennberg, P. O.: Atmospheric Fate of Methacrolein. 1. Peroxy Radical Isomerization Following Addition of OH and O$_2$, J. Phys. Chem. A, 116, 5756–5762, https://doi.org/10.1021/jp211560u, 2012.

Crounse, J. D., Nielsen, L. B., Jørgensen, S., Kjaergaard, H. G., and Wennberg, P. O.: Autoxidation of Organic Compounds in the Atmosphere, J. Phys. Chem. Lett., 4, 3513–3520, https://doi.org/10.1021/jz4019207, 2013.

Draper, D. C., Myllys, N., Hyttinen, N., Møller, K. H., Kjaergaard, H. G., Fry, J. L., Smith, J. N., and Kurten, T.: Formation of Highly Oxidized Molecules from NO$_3$ Radical Initiated Oxidation of Δ-3-Carene: A Mechanistic Study, ACS Earth and Space Chemistry, 3, 1460–1470, https://doi.org/10.1021/acsearthspacechem.9b00143, 2019.

Ehn, M., Thornton, J. A., Kleist, E., Sipila, M., Junninen, H., Pullinen, I., Springer, M., Rubach, F., Tillmann, R., Lee, B., Lopez-Hilfiker, F., Andres, S., Acir, I. H., Rissanen, M., Jokinen, T., Schobesberger, S., Kangasluoma, J., Kontkanen, J., Nieminen, T., Kurten, T., Nielsen, L. B., Jørgensen, S., Kjaergaard, H. G., Canagaratna, M., Dal Maso, M., Berndt, T., Petaja, T., Wahner, A., Kerminen, V. M., Kulmala, M., Worsnop, D. R., Wildt, J., and Mentel, T. F.: A large source of low-volatility secondary organic aerosol, Nature, 506, 476–479, https://doi.org/10.1038/nature13032, 2014.

Ehn, M., Berndt, T., Wildt, J., and Mentel, T.: Highly Oxygenated Molecules from Atmospheric Autoxidation of Hydrocarbons: A Prominent Challenge for Chemical Kinetics Studies, Int. J. Chem. Kinet., 49, 821–831, https://doi.org/10.1002/kin.21130, 2017.

Eisele, F. L. and Tanner, D. J.: Measurement of the gas phase concentration of H$_2$SO$_4$ and methane sulfonic acid and estimates of H$_2$SO$_4$ production and loss in the atmosphere, J. Geophys. Res.-Atmos., 98, 9001–9010, https://doi.org/10.1029/93jd00031, 1993.

Faxon, C., Hammes, J., Le Breton, M., Pathak, R. K., and Hallquist, M.: Characterization of organic nitrate constituents of secondary organic aerosol (SOA) from nitrate-radical-initiated oxidation of limonene using high-resolution chemical ionization mass spectrometry, Atmos. Chem. Phys., 18, 5467–5481, https://doi.org/10.5194/acp-18-5467-2018, 2018.

Finlayson-Pitts, B. and Pitts, J.: Chemistry of the upper and lower atmosphere, Academic Press, San Diego, 2000.

Fry, J. L., Kiendler-Scharr, A., Rollins, A. W., Wooldridge, P. J., Brown, S. S., Fuchs, H., Dubé, W., Mensah, A., dal Maso, M., Tillmann, R., Dorn, H.-P., Brauers, T., and Cohen, R. C.: Organic nitrate and secondary organic aerosol yield from NO$_3$ oxidation of β-pinene evaluated using a gas-phase kinetics/aerosol partitioning model, Atmos. Chem. Phys., 9, 1431–1449, https://doi.org/10.5194/acp-9-1431-2009, 2009.

Fry, J. L., Kiendler-Scharr, A., Rollins, A. W., Brauers, T., Brown, S. S., Dorn, H.-P., Dubé, W. P., Fuchs, H., Mensah, A., Rohrer, F., Tillmann, R., Wahner, A., Wooldridge, P. J., and Cohen, R. C.: SOA from limonene: role of NO$_3$ in its gen-

eration and degradation, Atmos. Chem. Phys., 11, 3879–3894, https://doi.org/10.5194/acp-11-3879-2011, 2011.

Fry, J. L., Draper, D. C., Barsanti, K. C., Smith, J. N., Ortega, J., Winkle, P. M., Lawler, M. J., Brown, S. S., Edwards, P. M., Cohen, R. C., and Lee, L.: Secondary Organic Aerosol Formation and Organic Nitrate Yield from NO_3 Oxidation of Biogenic Hydrocarbons, Environ. Sci. Technol., 48, 11944–11953, https://doi.org/10.1021/es502204x, 2014.

Fry, J. L., Brown, S. S., Middlebrook, A. M., Edwards, P. M., Campuzano-Jost, P., Day, D. A., Jimenez, J. L., Allen, H. M., Ryerson, T. B., Pollack, I., Graus, M., Warneke, C., de Gouw, J. A., Brock, C. A., Gilman, J., Lerner, B. M., Dubé, W. P., Liao, J., and Welti, A.: Secondary organic aerosol (SOA) yields from NO_3 radical + isoprene based on nighttime aircraft power plant plume transects, Atmos. Chem. Phys., 18, 11663–11682, https://doi.org/10.5194/acp-18-11663-2018, 2018.

Fuchs, H., Dorn, H.-P., Bachner, M., Bohn, B., Brauers, T., Gomm, S., Hofzumahaus, A., Holland, F., Nehr, S., Rohrer, F., Tillmann, R., and Wahner, A.: Comparison of OH concentration measurements by DOAS and LIF during SAPHIR chamber experiments at high OH reactivity and low NO concentration, Atmos. Meas. Tech., 5, 1611–1626, https://doi.org/10.5194/amt-5-1611-2012, 2012.

Garmash, O., Rissanen, M. P., Pullinen, I., Schmitt, S., Kausiala, O., Tillmann, R., Zhao, D., Percival, C., Bannan, T. J., Priestley, M., Hallquist, Å. M., Kleist, E., Kiendler-Scharr, A., Hallquist, M., Berndt, T., McFiggans, G., Wildt, J., Mentel, T. F., and Ehn, M.: Multi-generation OH oxidation as a source for highly oxygenated organic molecules from aromatics, Atmos. Chem. Phys., 20, 515–537, https://doi.org/10.5194/acp-20-515-2020, 2020.

Geyer, A., Alicke, B., Konrad, S., Schmitz, T., Stutz, J., and Platt, U.: Chemistry and oxidation capacity of the nitrate radical in the continental boundary layer near Berlin, J. Geophys. Res.-Atmos., 106, 8013–8025, https://doi.org/10.1029/2000jd900681, 2001.

Hamilton, J. F., Bryant, D. J., Edwards, P. M., Ouyang, B., Bannan, T. J., Mehra, A., Mayhew, A. W., Hopkins, J. R., Dunmore, R. E., Squires, F. A., Lee, J. D., Newland, M. J., Worrall, S. D., Bacak, A., Coe, H., Percival, C., Whalley, L. K., Heard, D. E., Slater, E. J., Jones, R. L., Cui, T., Surratt, J. D., Reeves, C. E., Mills, G. P., Grimmond, S., Sun, Y., Xu, W., Shi, Z., and Rickard, A. R.: Key Role of NO_3 Radicals in the Production of Isoprene Nitrates and Nitrooxyorganosulfates in Beijing, Environ. Sci. Technol., 55, 842–853, https://doi.org/10.1021/acs.est.0c05689, 2021.

Huang, W., Saathoff, H., Shen, X. L., Ramisetty, R., Leisner, T., and Mohr, C.: Chemical Characterization of Highly Functionalized Organonitrates Contributing to Night-Time Organic Aerosol Mass Loadings and Particle Growth, Environ. Sci. Technol., 53, 1165–1174, https://doi.org/10.1021/acs.est.8b05826, 2019.

Hyttinen, N., Kupiainen-Määttä, O., Rissanen, M. P., Muuronen, M., Ehn, M., and Kurtén, T.: Modeling the Charging of Highly Oxidized Cyclohexene Ozonolysis Products Using Nitrate-Based Chemical Ionization, J. Phys. Chem. A, 119, 6339–6345, https://doi.org/10.1021/acs.jpca.5b01818, 2015.

Japar, S. M. and Niki, H.: Gas-phase reactions of the nitrate radical with olefins, J. Phys. Chem., 79, 1629–1632, https://doi.org/10.1021/j100583a002, 1975.

Jenkin, M. E., Saunders, S. M., and Pilling, M. J.: The tropospheric degradation of volatile organic compounds: A proto-

col for mechanism development, Atmos. Environ., 31, 81–104, https://doi.org/10.1016/s1352-2310(96)00105-7, 1997.

Jenkin, M. E., Boyd, A. A., and Lesclaux, R.: Peroxy Radical Kinetics Resulting from the OH-Initiated Oxidation of 1,3-Butadiene, 2,3-Dimethyl-1,3-Butadiene and Isoprene, J. Atmos. Chem., 29, 267–298, https://doi.org/10.1023/A:1005940332441, 1998.

Jenkin, M. E., Saunders, S. M., Wagner, V., and Pilling, M. J.: Protocol for the development of the Master Chemical Mechanism, MCM v3 (Part B): tropospheric degradation of aromatic volatile organic compounds, Atmos. Chem. Phys., 3, 181–193, https://doi.org/10.5194/acp-3-181-2003, 2003.

Jenkin, M. E., Young, J. C., and Rickard, A. R.: The MCM v3.3.1 degradation scheme for isoprene, Atmos. Chem. Phys., 15, 11433–11459, https://doi.org/10.5194/acp-15-11433-2015, 2015.

Jokinen, T., Sipilä, M., Junninen, H., Ehn, M., Lönn, G., Hakala, J., Petäjä, T., Mauldin III, R. L., Kulmala, M., and Worsnop, D. R.: Atmospheric sulphuric acid and neutral cluster measurements using CI-APi-TOF, Atmos. Chem. Phys., 12, 4117–4125, https://doi.org/10.5194/acp-12-4117-2012, 2012.

Jokinen, T., Sipila, M., Richters, S., Kerminen, V. M., Paasonen, P., Stratmann, F., Worsnop, D., Kulmala, M., Ehn, M., Herrmann, H., and Berndt, T.: Rapid Autoxidation Forms Highly Oxidized RO_2 Radicals in the Atmosphere, Angew. Chem.-Int. Edit., 53, 14596–14600, https://doi.org/10.1002/anie.201408566, 2014.

Jokinen, T., Berndt, T., Makkonen, R., Kerminen, V. M., Junninen, H., Paasonen, P., Stratmann, F., Herrmann, H., Guenther, A. B., Worsnop, D. R., Kulmala, M., Ehn, M., and Sipila, M.: Production of extremely low volatile organic compounds from biogenic emissions: Measured yields and atmospheric implications, P. Natl. Acad. Sci. USA, 112, 7123–7128, https://doi.org/10.1073/pnas.1423977112, 2015.

Kaminski, M., Fuchs, H., Acir, I.-H., Bohn, B., Brauers, T., Dorn, H.-P., Häseler, R., Hofzumahaus, A., Li, X., Lutz, A., Nehr, S., Rohrer, F., Tillmann, R., Vereecken, L., Wegener, R., and Wahner, A.: Investigation of the β-pinene photooxidation by OH in the atmosphere simulation chamber SAPHIR, Atmos. Chem. Phys., 17, 6631–6650, https://doi.org/10.5194/acp-17-6631-2017, 2017.

Kenseth, C. M., Huang, Y. L., Zhao, R., Dalleska, N. F., Hethcox, C., Stoltz, B. M., and Seinfeld, J. H.: Synergistic O_3 + OH oxidation pathway to extremely low-volatility dimers revealed in beta-pinene secondary organic aerosol, P. Natl. Acad. Sci. USA, 115, 8301–8306, https://doi.org/10.1073/pnas.1804671115, 2018.

Kirkby, J., Duplissy, J., Sengupta, K., Frege, C., Gordon, H., Williamson, C., Heinritzi, M., Simon, M., Yan, C., Almeida, J., Tröstl, J., Nieminen, T., Ortega, I. K., Wagner, R., Adamov, A., Amorim, A., Bernhammer, A.-K., Bianchi, F., Breitenlechner, M., Brilke, S., Chen, X., Craven, J., Dias, A., Ehrhart, S., Flagan, R. C., Franchin, A., Fuchs, C., Guida, R., Hakala, J., Hoyle, C. R., Jokinen, T., Junninen, H., Kangasluoma, J., Kim, J., Krapf, M., Kürten, A., Laaksonen, A., Lehtipalo, K., Makhmutov, V., Mathot, S., Molteni, U., Onnela, A., Peräkylä, O., Piel, F., Petäjä, T., Praplan, A. P., Pringle, K., Rap, A., Richards, N. A. D., Riipinen, I., Rissanen, M. P., Rondo, L., Sarnela, N., Schobesberger, S., Scott, C. E., Seinfeld, J. H., Sipilä, M., Steiner, G., Stozhkov, Y., Stratmann, F., Tomé, A., Virtanen, A., Vogel, A. L., Wagner, A. C., Wagner, P. E., Weingartner, E., Wimmer, D., Winkler, P. M., Ye, P., Zhang, X., Hansel, A., Dommen, J., Donahue, N.

M., Worsnop, D. R., Baltensperger, U., Kulmala, M., Carslaw, K. S., and Curtius, J.: Ion-induced nucleation of pure biogenic particles, Nature, 533, 521–526, https://doi.org/10.1038/nature17953, 2016.

Krechmer, J. E., Coggon, M. M., Massoli, P., Nguyen, T. B., Crounse, J. D., Hu, W. W., Day, D. A., Tyndall, G. S., Henze, D. K., Rivera-Rios, J. C., Nowak, J. B., Kimmel, J. R., Mauldin, R. L., Stark, H., Jayne, J. T., Sipila, M., Junninen, H., St Clair, J. M., Zhang, X., Feiner, P. A., Zhang, L., Miller, D. O., Brune, W. H., Keutsch, F. N., Wennberg, P. O., Seinfeld, J. H., Worsnop, D. R., Jimenez, J. L., and Canagaratna, M. R.: Formation of Low Volatility Organic Compounds and Secondary Organic Aerosol from Isoprene Hydroxyhydroperoxide Low-NO Oxidation, Environ. Sci. Technol., 49, 10330–10339, https://doi.org/10.1021/acs.est.5b02031, 2015.

Kwan, A. J., Chan, A. W. H., Ng, N. L., Kjaergaard, H. G., Seinfeld, J. H., and Wennberg, P. O.: Peroxy radical chemistry and OH radical production during the NO$_3$-initiated oxidation of isoprene, Atmos. Chem. Phys., 12, 7499–7515, https://doi.org/10.5194/acp-12-7499-2012, 2012.

Lai, C. C. and Finlayson-Pitts, B. J.: Reactions of dinitrogen pentoxide and nitrogen-dioxide with 1-palmitoyl-2-oleoyl-*sn*-glycero-3-phosphocholine, Lipids, 26, 306–314, https://doi.org/10.1007/bf02537142, 1991.

Lee, B. H., Mohr, C., Lopez-Hilfiker, F. D., Lutz, A., Hallquist, M., Lee, L., Romer, P., Cohen, R. C., Iyer, S., Kurten, T., Hu, W., Day, D. A., Campuzano-Jost, P., Jimenez, J. L., Xu, L., Ng, N. L., Guo, H., Weber, R. J., Wild, R. J., Brown, S. S., Koss, A., de Gouw, J., Olson, K., Goldstein, A. H., Seco, R., Kim, S., McAvey, K., Shepson, P. B., Starn, T., Baumann, K., Edgerton, E. S., Liu, J., Shilling, J. E., Miller, D. O., Brune, W., Schobesberger, S., D'Ambro, E. L., and Thornton, J. A.: Highly functionalized organic nitrates in the southeast United States: Contribution to secondary organic aerosol and reactive nitrogen budgets, P. Natl. Acad. Sci. USA, 113, 1516–1521, https://doi.org/10.1073/pnas.1508108113, 2016.

Lu, K. D., Rohrer, F., Holland, F., Fuchs, H., Brauers, T., Oebel, A., Dlugi, R., Hu, M., Li, X., Lou, S. R., Shao, M., Zhu, T., Wahner, A., Zhang, Y. H., and Hofzumahaus, A.: Nighttime observation and chemistry of HO$_x$ in the Pearl River Delta and Beijing in summer 2006, Atmos. Chem. Phys., 14, 4979–4999, https://doi.org/10.5194/acp-14-4979-2014, 2014.

Malkin, T. L., Goddard, A., Heard, D. E., and Seakins, P. W.: Measurements of OH and HO$_2$ yields from the gas phase ozonolysis of isoprene, Atmos. Chem. Phys., 10, 1441–1459, https://doi.org/10.5194/acp-10-1441-2010, 2010.

Massoli, P., Stark, H., Canagaratna, M. R., Krechmer, J. E., Xu, L., Ng, N. L., Mauldin, R. L., Yan, C., Kimmel, J., Misztal, P. K., Jimenez, J. L., Jayne, J. T., and Worsnop, D. R.: Ambient Measurements of Highly Oxidized Gas-Phase Molecules during the Southern Oxidant and Aerosol Study (SOAS) 2013, ACS Earth and Space Chemistry, 2, 653–672, https://doi.org/10.1021/acsearthspacechem.8b00028, 2018.

McFiggans, G., Mentel, T. F., Wildt, J., Pullinen, I., Kang, S., Kleist, E., Schmitt, S., Springer, M., Tillmann, R., Wu, C., Zhao, D., Hallquist, M., Faxon, C., Le Breton, M., Hallquist, Å. M., Simpson, D., Bergström, R., Jenkin, M. E., Ehn, M., Thornton, J. A., Alfarra, M. R., Bannan, T. J., Percival, C. J., Priestley, M., Topping, D., and Kiendler-Scharr, A.: Secondary organic aerosol re-

duced by mixture of atmospheric vapours, Nature, 565, 587–593, https://doi.org/10.1038/s41586-018-0871-y, 2019.

Mentel, T. F., Springer, M., Ehn, M., Kleist, E., Pullinen, I., Kurtén, T., Rissanen, M., Wahner, A., and Wildt, J.: Formation of highly oxidized multifunctional compounds: autoxidation of peroxy radicals formed in the ozonolysis of alkenes – deduced from structure–product relationships, Atmos. Chem. Phys., 15, 6745–6765, https://doi.org/10.5194/acp-15-6745-2015, 2015.

Møller, K. H., Bates, K. H., and Kjaergaard, H. G.: The Importance of Peroxy Radical Hydrogen-Shift Reactions in Atmospheric Isoprene Oxidation, J. Phys. Chem. A, 123, 920–932, https://doi.org/10.1021/acs.jpca.8b10432, 2019.

Molteni, U., Bianchi, F., Klein, F., El Haddad, I., Frege, C., Rossi, M. J., Dommen, J., and Baltensperger, U.: Formation of highly oxygenated organic molecules from aromatic compounds, Atmos. Chem. Phys., 18, 1909–1921, https://doi.org/10.5194/acp-18-1909-2018, 2018.

Molteni, U., Simon, M., Heinritzi, M., Hoyle, C. R., Bernhammer, A. K., Bianchi, F., Breitenlechner, M., Brilke, S., Dias, A., Duplissy, J., Frege, C., Gordon, H., Heyn, C., Jokinen, T., Kurten, A., Lehtipalo, K., Makhmutov, V., Petaja, T., Pieber, S. M., Praplan, A. P., Schobesberger, S., Steiner, G., Stozhkov, Y., Tome, A., Trostl, J., Wagner, A. C., Wagner, R., Williamson, C., Yan, C., Baltensperger, U., Curtius, J., Donahue, N. M., Hansel, A., Kirkby, J., Kulmala, M., Worsnop, D. R., and Dommen, J.: Formation of Highly Oxygenated Organic Molecules from alpha-Pinene Ozonolysis: Chemical Characteristics, Mechanism, and Kinetic Model Development, Acs Earth and Space Chemistry, 3, 873–883, https://doi.org/10.1021/acsearthspacechem.9b00035, 2019.

Nah, T., Sanchez, J., Boyd, C. M., and Ng, N. L.: Photochemical Aging of alpha-pinene and beta-pinene Secondary Organic Aerosol formed from Nitrate Radical Oxidation, Environ. Sci. Technol., 50, 222–231, https://doi.org/10.1021/acs.est.5b04594, 2016.

Ng, N. L., Kwan, A. J., Surratt, J. D., Chan, A. W. H., Chhabra, P. S., Sorooshian, A., Pye, H. O. T., Crounse, J. D., Wennberg, P. O., Flagan, R. C., and Seinfeld, J. H.: Secondary organic aerosol (SOA) formation from reaction of isoprene with nitrate radicals (NO$_3$), Atmos. Chem. Phys., 8, 4117–4140, https://doi.org/10.5194/acp-8-4117-2008, 2008.

Nguyen, T. B., Tyndall, G. S., Crounse, J. D., Teng, A. P., Bates, K. H., Schwantes, R. H., Coggon, M. M., Zhang, L., Feiner, P., Milller, D. O., Skog, K. M., Rivera-Rios, J. C., Dorris, M., Olson, K. F., Koss, A., Wild, R. J., Brown, S. S., Goldstein, A. H., de Gouw, J. A., Brune, W. H., Keutsch, F. N., Seinfeld, J. H., and Wennberg, P. O.: Atmospheric fates of Criegee intermediates in the ozonolysis of isoprene, Phys. Chem. Chem. Phys., 18, 10241–10254, https://doi.org/10.1039/c6cp00053c, 2016.

Novelli, A., Cho, C., Fuchs, H., Hofzumahaus, A., Rohrer, F., Tillmann, R., Kiendler-Scharr, A., Wahner, A., and Vereecken, L.: Experimental and theoretical study on the impact of a nitrate group on the chemistry of alkoxy radicals, Phys. Chem. Chem. Phys., 23, 5474–5495, https://doi.org/10.1039/D0CP05555G, 2021.

Nozière, B. and Vereecken, L.: Direct Observation of Aliphatic Peroxy Radical Autoxidation and Water Effects: An Experimental and Theoretical Study, Angew. Chem.-Int. Edit., 58, 13976–13982, https://doi.org/10.1002/anie.201907981, 2019.

Perring, A. E., Wisthaler, A., Graus, M., Wooldridge, P. J., Lockwood, A. L., Mielke, L. H., Shepson, P. B., Hansel, A., and Cohen, R. C.: A product study of the isoprene+NO$_3$ reaction, Atmos. Chem. Phys., 9, 4945–4956, https://doi.org/10.5194/acp-9-4945-2009, 2009.

Pfrang, C., Martin, R. S., Canosa-Mas, C. E., and Wayne, R. P.: Gas-phase reactions of NO$_3$ and N$_2$O$_5$ with (Z)-hex-4-en-1-ol, (Z)-hex-3-en-1-ol ('leaf alcohol'), (E)-hex-3-en-1-ol, (Z)-hex-2-en-1-ol and (E)-hex-2-en-1-ol, Phys. Chem. Chem. Phys., 8, 354–363, https://doi.org/10.1039/b510835g, 2006.

Pullinen, I., Schmitt, S., Kang, S., Sarrafzadeh, M., Schlag, P., Andres, S., Kleist, E., Mentel, T. F., Rohrer, F., Springer, M., Tillmann, R., Wildt, J., Wu, C., Zhao, D., Wahner, A., and Kiendler-Scharr, A.: Impact of NO$_x$ on secondary organic aerosol (SOA) formation from α-pinene and β-pinene photooxidation: the role of highly oxygenated organic nitrates, Atmos. Chem. Phys., 20, 10125–10147, https://doi.org/10.5194/acp-20-10125-2020, 2020.

Quéléver, L. L. J., Kristensen, K., Normann Jensen, L., Rosati, B., Teiwes, R., Daellenbach, K. R., Peräkylä, O., Roldin, P., Bossi, R., Pedersen, H. B., Glasius, M., Bilde, M., and Ehn, M.: Effect of temperature on the formation of highly oxygenated organic molecules (HOMs) from alpha-pinene ozonolysis, Atmos. Chem. Phys., 19, 7609–7625, https://doi.org/10.5194/acp-19-7609-2019, 2019.

Richters, S., Pfeifle, M., Olzmann, M., and Berndt, T.: endo-Cyclization of unsaturated RO$_2$ radicals from the gas-phase ozonolysis of cyclohexadienes, Chem. Commun., 53, 4132–4135, https://doi.org/10.1039/c7cc01350g, 2017.

Rissanen, M. P., Kurten, T., Sipila, M., Thornton, J. A., Kangasluoma, J., Sarnela, N., Junninen, H., Jørgensen, S., Schallhart, S., Kajos, M. K., Taipale, R., Springer, M., Mentel, T. F., Ruuskanen, T., Petaja, T., Worsnop, D. R., Kjaergaard, H. G., and Ehn, M.: The Formation of Highly Oxidized Multifunctional Products in the Ozonolysis of Cyclohexene, J. Am. Chem. Soc., 136, 15596–15606, https://doi.org/10.1021/ja507146s, 2014.

Rissanen, M. P., Kurten, T., Sipila, M., Thornton, J. A., Kausiala, O., Garmash, O., Kjaergaard, H. G., Petaja, T., Worsnop, D. R., Ehn, M., and Kulmala, M.: Effects of Chemical Complexity on the Autoxidation Mechanisms of Endocyclic Alkene Ozonolysis Products: From Methylcyclohexenes toward Understanding alpha-Pinene, J. Phys. Chem. A, 119, 4633–4650, https://doi.org/10.1021/jp510966g, 2015.

Riva, M., Rantala, P., Krechmer, J. E., Peräkylä, O., Zhang, Y., Heikkinen, L., Garmash, O., Yan, C., Kulmala, M., Worsnop, D., and Ehn, M.: Evaluating the performance of five different chemical ionization techniques for detecting gaseous oxygenated organic species, Atmos. Meas. Tech., 12, 2403–2421, https://doi.org/10.5194/amt-12-2403-2019, 2019.

Rohrer, F., Bohn, B., Brauers, T., Brüning, D., Johnen, F.-J., Wahner, A., and Kleffmann, J.: Characterisation of the photolytic HONO-source in the atmosphere simulation chamber SAPHIR, Atmos. Chem. Phys., 5, 2189–2201, https://doi.org/10.5194/acp-5-2189-2005, 2005.

Rollins, A. W., Kiendler-Scharr, A., Fry, J. L., Brauers, T., Brown, S. S., Dorn, H.-P., Dubé, W. P., Fuchs, H., Mensah, A., Mentel, T. F., Rohrer, F., Tillmann, R., Wegener, R., Wooldridge, P. J., and Cohen, R. C.: Isoprene oxidation by nitrate radical: alkyl nitrate

and secondary organic aerosol yields, Atmos. Chem. Phys., 9, 6685–6703, https://doi.org/10.5194/acp-9-6685-2009, 2009.

Saunders, S. M., Jenkin, M. E., Derwent, R. G., and Pilling, M. J.: Protocol for the development of the Master Chemical Mechanism, MCM v3 (Part A): tropospheric degradation of non-aromatic volatile organic compounds, Atmos. Chem. Phys., 3, 161–180, https://doi.org/10.5194/acp-3-161-2003, 2003.

Schwantes, R. H., Teng, A. P., Nguyen, T. B., Coggon, M. M., Crounse, J. D., St Clair, J. M., Zhang, X., Schilling, K. A., Seinfeld, J. H., and Wennberg, P. O.: Isoprene NO$_3$ Oxidation Products from the RO$_2$+HO$_2$ Pathway, J. Phys. Chem. A 119, 10158–10171, https://doi.org/10.1021/acs.jpca.5b06355, 2015.

Skov, H., Hjorth, J., Lohse, C., Jensen, N. R., and Restelli, G.: Products and mechanisms of the reactions of the nitrate radical (NO$_3$) with isoprene, 1,3-butadiene and 2,3-dimethyl-1,3-butadiene in air, Atmos. Environ. A.-Gen., 26, 2771–2783, https://doi.org/10.1016/0960-1686(92)90015-D, 1992.

Stark, M. S.: Epoxidation of Alkenes by Peroxyl Radicals in the Gas Phase: Structure-Activity Relationships, J. Phys. Chem. A, 101, 8296–8301, https://doi.org/10.1021/jp972054+, 1997.

Stark, M. S.: Addition of Peroxyl Radicals to Alkenes and the Reaction of Oxygen with Alkyl Radicals, J. Am. Chem. Soc., 122, 4162–4170, https://doi.org/10.1021/ja993760m, 2000.

Starn, T. K., Shepson, P. B., Bertman, S. B., Riemer, D. D., Zika, R. G., and Olszyna, K.: Nighttime isoprene chemistry at an urban-impacted forest site, 103, 22437–22447, https://doi.org/10.1029/98JD01201, 1998.

Stroud, C. A., Roberts, J. M., Williams, E. J., Hereid, D., Angevine, W. M., Fehsenfeld, F. C., Wisthaler, A., Hansel, A., Martinez-Harder, M., Harder, H., Brune, W. H., Hoenninger, G., Stutz, J., and White, A. B.: Nighttime isoprene trends at an urban forested site during the 1999 Southern Oxidant Study, 107, ACH 7-1–ACH 7-14, https://doi.org/10.1029/2001JD000959, 2002.

Takeuchi, M. and Ng, N. L.: Chemical composition and hydrolysis of organic nitrate aerosol formed from hydroxyl and nitrate radical oxidation of α-pinene and β-pinene, Atmos. Chem. Phys., 19, 12749–12766, https://doi.org/10.5194/acp-19-12749-2019, 2019.

Tan, Z., Lu, K., Hofzumahaus, A., Fuchs, H., Bohn, B., Holland, F., Liu, Y., Rohrer, F., Shao, M., Sun, K., Wu, Y., Zeng, L., Zhang, Y., Zou, Q., Kiendler-Scharr, A., Wahner, A., and Zhang, Y.: Experimental budgets of OH, HO$_2$, and RO$_2$ radicals and implications for ozone formation in the Pearl River Delta in China 2014, Atmos. Chem. Phys., 19, 7129–7150, https://doi.org/10.5194/acp-19-7129-2019, 2019.

Tröstl, J., Chuang, W. K., Gordon, H., Heinritzi, M., Yan, C., Molteni, U., Ahlm, L., Frege, C., Bianchi, F., Wagner, R., Simon, M., Lehtipalo, K., Williamson, C., Craven, J. S., Duplissy, J., Adamov, A., Almeida, J., Bernhammer, A.-K., Breitenlechner, M., Brilke, S., Dias, A., Ehrhart, S., Flagan, R. C., Franchin, A., Fuchs, C., Guida, R., Gysel, M., Hansel, A., Hoyle, C. R., Jokinen, T., Junninen, H., Kangasluoma, J., Keskinen, H., Kim, J., Krapf, M., Kürten, A., Laaksonen, A., Lawler, M., Leiminger, M., Mathot, S., Möhler, O., Nieminen, T., Onnela, A., Petäjä, T., Piel, F. M., Miettinen, P., Rissanen, M. P., Rondo, L., Sarnela, N., Schobesberger, S., Sengupta, K., Sipilä, M., Smith, J. N., Steiner, G., Tomè, A., Virtanen, A., Wagner, A. C., Weingartner, E., Wimmer, D., Winkler, P. M., Ye, P., Carslaw, K. S., Curtius, J., Dommen, J., Kirkby, J., Kulmala,

M., Riipinen, I., Worsnop, D. R., Donahue, N. M., and Baltensperger, U.: The role of low-volatility organic compounds in initial particle growth in the atmosphere, Nature, 533, 527–531, https://doi.org/10.1038/nature18271, 2016.

Valiev, R. R., Hasan, G., Salo, V.-T., Kubecka, J., and Kurten, T.: Intersystem Crossings Drive Atmospheric Gas-Phase Dimer Formation, J. Phys. Chem. A, 123, 6596–6604, https://doi.org/10.1021/acs.jpca.9b02559, 2019.

Vereecken, L. and Francisco, J. S.: Theoretical studies of atmospheric reaction mechanisms in the troposphere, Chem. Soc. Rev., 41, 6259–6293, https://doi.org/10.1039/c2cs35070j, 2012.

Vereecken, L. and Nozière, B.: H migration in peroxy radicals under atmospheric conditions, Atmos. Chem. Phys., 20, 7429–7458, https://doi.org/10.5194/acp-20-7429-2020, 2020.

Vereecken, L. and Peeters, J.: Nontraditional (per)oxy ring-closure paths in the atmospheric oxidation of isoprene and monoterpenes, J. Phys. Chem. A, 108, 5197–5204, https://doi.org/10.1021/jp049219g, 2004.

Vereecken, L. and Peeters, J.: A structure-activity relationship for the rate coefficient of H-migration in substituted alkoxy radicals, Phys. Chem. Chem. Phys., 12, 12608–12620, https://doi.org/10.1039/c0cp00387e, 2010.

Vereecken, L. and Peeters, J.: A theoretical study of the OH-initiated gas-phase oxidation mechanism of beta-pinene $(C_{10}H_{16})$: first generation products, Phys. Chem. Chem. Phys., 14, 3802–3815, https://doi.org/10.1039/c2cp23711c, 2012.

Vereecken, L., Mueller, J. F., and Peeters, J.: Low-volatility poly-oxygenates in the OH-initiated atmospheric oxidation of alpha-pinene: impact of non-traditional peroxyl radical chemistry, Phys. Chem. Chem. Phys., 9, 5241–5248, https://doi.org/10.1039/b708023a, 2007.

Vereecken, L., Carlsson, P. T. M., Novelli, A., Bernard, F., Brown, S. S., Cho, C., Crowley, J. N., Fuchs, H., Mellouki, W., Reimer, D., Shenolikar, J., Tillmann, R., Zhou, L., Kiendler-Scharr, A., and Wahner, A.: Theoretical and experimental study of peroxy and alkoxy radicals in the NO_3-initiated oxidation of isoprene, Phys. Chem. Chem. Phys., 23, 5496–5515, https://doi.org/10.1039/d0cp06267g, 2021.

Viggiano, A. A., Seeley, J. V., Mundis, P. L., Williamson, J. S., and Morris, R. A.: Rate Constants for the Reactions of $XO_3^-(H_2O)_n$ $(X = C, HC, and N)$ and $NO_3^-(HNO_3)_n$ with H_2SO_4: Implications for Atmospheric Detection of H_2SO_4, J. Phys. Chem. A, 101, 8275–8278, https://doi.org/10.1021/jp971768h, 1997.

Wagner, N. L., Dubé, W. P., Washenfelder, R. A., Young, C. J., Pollack, I. B., Ryerson, T. B., and Brown, S. S.: Diode laser-based cavity ring-down instrument for NO_3, N_2O_5, NO, NO_2 and O_3 from aircraft, Atmos. Meas. Tech., 4, 1227–1240, https://doi.org/10.5194/amt-4-1227-2011, 2011.

Wang, Y., Mehra, A., Krechmer, J. E., Yang, G., Hu, X., Lu, Y., Lambe, A., Canagaratna, M., Chen, J., Worsnop, D., Coe, H., and Wang, L.: Oxygenated products formed from OH-initiated reactions of trimethylbenzene: autoxidation and accretion, Atmos. Chem. Phys., 20, 9563–9579, https://doi.org/10.5194/acp-20-9563-2020, 2020.

Wennberg, P. O., Bates, K. H., Crounse, J. D., Dodson, L. G., McVay, R. C., Mertens, L. A., Nguyen, T. B., Praske, E., Schwantes, R. H., Smarte, M. D., St Clair, J. M., Teng, A. P., Zhang, X., and Seinfeld, J. H.: Gas-Phase Reactions of Isoprene and

Its Major Oxidation Products, Chem. Rev., 118, 3337–3390, https://doi.org/10.1021/acs.chemrev.7b00439, 2018.

Wu, R., Vereecken, L., Tsiligiannis, E., Kang, S., Albrecht, S. R., Hantschke, L., Zhao, D., Novelli, A., Fuchs, H., Tillmann, R., Hohaus, T., Carlsson, P. T. M., Shenolikar, J., Bernard, F., Crowley, J. N., Fry, J. L., Brownwood, B., Thornton, J. A., Brown, S. S., Kiendler-Scharr, A., Wahner, A., Hallquist, M., and Mentel, T. F.: Molecular composition and volatility of multi-generation products formed from isoprene oxidation by nitrate radical, Atmos. Chem. Phys. Discuss. [preprint], https://doi.org/10.5194/acp-2020-1180, in review, 2020. TS3

Xu, L., Guo, H. Y., Boyd, C. M., Klein, M., Bougiatioti, A., Cerully, K. M., Hite, J. R., Isaacman-VanWertz, G., Kreisberg, N. M., Knote, C., Olson, K., Koss, A., Goldstein, A. H., Hering, S. V., de Gouw, J., Baumann, K., Lee, S. H., Nenes, A., Weber, R. J., and Ng, N. L.: Effects of anthropogenic emissions on aerosol formation from isoprene and monoterpenes in the southeastern United States, P. Natl. Acad. Sci. USA, 112, 37–42, https://doi.org/10.1073/pnas.1417609112, 2015.

Xu, Z. N., Nie, W., Liu, Y. L., Sun, P., Huang, D. D., Yan, C., Krechmer, J., Ye, P. L., Xu, Z., Qi, X. M., Zhu, C. J., Li, Y. Y., Wang, T. Y., Wang, L., Huang, X., Tang, R. Z., Guo, S., Xiu, G. L., Fu, Q. Y., Worsnop, D., Chi, X. G., and Ding, A. J.: Multifunctional Products of Isoprene Oxidation in Polluted Atmosphere and Their Contribution to SOA, Geophys. Res. Lett., 48, e2020GL089276, https://doi.org/10.1029/2020GL089276, 2021.

Yan, C., Nie, W., Äijälä, M., Rissanen, M. P., Canagaratna, M. R., Massoli, P., Junninen, H., Jokinen, T., Sarnela, N., Häme, S. A. K., Schobesberger, S., Canonaco, F., Yao, L., Prévôt, A. S. H., Petäjä, T., Kulmala, M., Sipilä, M., Worsnop, D. R., and Ehn, M.: Source characterization of highly oxidized multifunctional compounds in a boreal forest environment using positive matrix factorization, Atmos. Chem. Phys., 16, 12715–12731, https://doi.org/10.5194/acp-16-12715-2016, 2016.

Yan, C., Nie, W., Vogel, A. L., Dada, L., Lehtipalo, K., Stolzenburg, D., Wagner, R., Rissanen, M. P., Xiao, M., Ahonen, L., Fischer, L., Rose, C., Bianchi, F., Gordon, H., Simon, M., Heinritzi, M., Garmash, O., Roldin, P., Dias, A., Ye, P., Hofbauer, V., Amorim, A., Bauer, P. S., Bergen, A., Bernhammer, A. K., Breitenlechner, M., Brilke, S., Buchholz, A., Mazon, S. B., Canagaratna, M. R., Chen, X., Ding, A., Dommen, J., Draper, D. C., Duplissy, J., Frege, C., Heyn, C., Guida, R., Hakala, J., Heikkinen, L., Hoyle, C. R., Jokinen, T., Kangasluoma, J., Kirkby, J., Kontkanen, J., Kurten, A., Lawler, M. J., Mai, H., Mathot, S., Mauldin, R. L., Molteni, U., Nichman, L., Nieminen, T., Nowak, J., Ojdanic, A., Onnela, A., Pajunoja, A., Petaja, T., Piel, F., Quelever, L. L. J., Sarnela, N., Schallhart, S., Sengupta, K., Sipila, M., Tome, A., Trostl, J., Vaisanen, O., Wagner, A. C., Ylisirnio, A., Zha, Q., Baltensperger, U., Carslaw, K. S., Curtius, J., Flagan, R. C., Hansel, A., Riipinen, I., Smith, J. N., Virtanen, A., Winkler, P. M., Donahue, N. M., Kerminen, V. M., Kulmala, M., Ehn, M., and Worsnop, D. R.: Size-dependent influence of NO_x on the growth rates of organic aerosol particles, Science Advances, 6, eaay4945, https://doi.org/10.1126/sciadv.aay4945, 2020.

Zhao, D., Schmitt, S. H., Wang, M., Acir, I.-H., Tillmann, R., Tan, Z., Novelli, A., Fuchs, H., Pullinen, I., Wegener, R., Rohrer, F., Wildt, J., Kiendler-Scharr, A., Wahner, A., and Mentel, T. F.: Effects of NO_x and SO_2 on the secondary organic aerosol formation from photooxidation of α-pinene and limonene, At-

mos. Chem. Phys., 18, 1611–1628, https://doi.org/10.5194/acp-18-1611-2018, 2018.

Zhao, D. F., Buchholz, A., Kortner, B., Schlag, P., Rubach, F., Kiendler-Scharr, A., Tillmann, R., Wahner, A., Flores, J. M., Rudich, Y., Watne, Å. K., Hallquist, M., Wildt, J., and Mentel, T. F.: Size-dependent hygroscopicity parameter (κ) and chemical composition of secondary organic cloud condensation nuclei, Geophys. Res. Lett., 42, 10920–10928, https://doi.org/10.1002/2015gl066497, 2015a.

Zhao, D. F., Kaminski, M., Schlag, P., Fuchs, H., Acir, I.-H., Bohn, B., Häseler, R., Kiendler-Scharr, A., Rohrer, F., Tillmann, R., Wang, M. J., Wegener, R., Wildt, J., Wahner, A., and Mentel, Th. F.: Secondary organic aerosol formation from hydroxyl radical oxidation and ozonolysis of monoterpenes, Atmos. Chem. Phys., 15, 991–1012, https://doi.org/10.5194/acp-15-991-2015, 2015b.

Ziemann, P. J. and Atkinson, R.: Kinetics, products, and mechanisms of secondary organic aerosol formation, Chem. Soc. Rev., 41, 6582–6605, https://doi.org/10.1039/c2cs35122f, 2012.

Remarks from the typesetter

TS1   Please check the link and confirm date of last access.

TS2   Please give an explanation of why this needs to be changed. We have to ask the handling editor for approval. Thanks.

TS3   Thank you for your update. Since the citation information has not changed into "accepted" on the website, this has to be cited accordingly.